Published in final edited form as:
J Med Chem. 2013 July 11; 56(13): . doi:10.1021/jm400707f.

Synthesis and evaluation of hetero- and homo-dimers of ribosome-targeting antibiotics: Antimicrobial activity, *in vitro* inhibition of translation, and drug resistance

Yifat Berkov-Zrihen[†], **Keith D. Green**[‡,§], **Kristin J. Labby**[‡], **Mark Feldman**[†], **Sylvie Garneau-Tsodikova**[*,‡,§], and **Micha Fridman**[*,†]

[†]School of Chemistry, Tel Aviv University, Tel Aviv, 6997801, Israel

[‡]Department of Medicinal Chemistry and the Life Sciences Institute, University of Michigan, Ann Arbor, Michigan, 48109, United States

Abstract

In this study, we describe the synthesis of a full set of homo- and hetero-dimers of three intact structures of different ribosome-targeting antibiotics: tobramycin, clindamycin, and chloramphenicol. Several aspects of the biological activity of the dimeric structures were evaluated including antimicrobial activity, inhibition of *in vitro* bacterial protein translation, and the effect of dimerization on the action of several bacterial resistance mechanisms that deactivate tobramycin and chloramphenicol. This study demonstrates that covalently linking two identical or different ribosome-targeting antibiotics may lead to (i) a broader spectrum of antimicrobial activity, (ii) improved inhibition of bacterial translation properties compared to that of the parent antibiotics, and (iii) reduction in the efficacy of some drug-modifying enzymes that confer high levels of resistance to the parent antibiotics from which the dimers were derived.

Keywords

Ribosome-targeting antimicrobials; Antibiotic hybrids; Drug resistance; Drug-modifying enzymes

INTRODUCTION

Protein biosynthesis is one of the fundamental processes required for all living cells, and the prokaryotic ribosome is a target of a large number of clinically useful antibiotics.[1–4] Bacterial ribosome-targeting antibiotics inhibit protein synthesis by interfering with the process of messenger RNA translation or by preventing the formation of peptide bond of the nascent protein. These effects result from the binding of these antibiotics to the aminoacyl-

[*]**Corresponding Author**, sylviegtsodikova@uky.edu or mfridman@post.tau.ac.il.
[§]Current address: Department of Pharmaceutical Sciences, University of Kentucky, Lexington, Kentucky, 40536, United States

ASSOCIATED CONTENT

Supporting Information. ^{1}H and ^{13}C NMR spectra of all new compounds synthesized as well as a Coomassie blue-stained SDS-PAGE gel showing the purified CTP and CNR are provided. A table of relative activity for tobramycin and chloramphenicol derivatives compared to the parent drugs against drug-modifying enzymes is also provided. This material is available free of charge via the Internet at http://pubs.acs.org.

Author Contributions

Yifat Berkov-Zrihen, Keith D. Green, Kristin J. Labby, and Mark Feldman designed and performed experiments and analyzed data. Micha Fridman and Sylvie Garneau-Tsodikova designed experiments, analyzed data, made final figures, and wrote the manuscript. All authors have given approval to the final version of the manuscript.

The authors declare no competing financial interest.

tRNA binding domain (A-site),[5–7] to the peptidyltransferase domain (P-site),[8–10] or to elements on both sites.[10]

Prolonged and inappropriate use of the various bacterial ribosome-targeting antibiotics enhanced the evolution of several bacterial resistance mechanisms that can be divided into four types: (i) inactivation through enzymatic modifications,[11] (ii) reduction in intracellular concentration through efflux pump proteins,[12, 13] (iii) reduction in membrane permeability,[14] and (iv) structural modifications in the ribosomal target sites.[15] Amongst ribosomal target modifications that lead to antibiotic resistance are mutations in rRNA, mutations in ribosomal proteins, and rRNA methylation catalyzed by several rRNA methyltransferases.[16–18]

The development of covalently linked dimers composed of intact clinically used antibiotics that inhibit similar or different bacterial targets has been widely explored.[19–21] The potential benefits of this strategy include the possibility of an expanded spectrum of activity, reduced potential for development of bacterial resistance, and an increase in specificity for bacterial cells that leads to reduced toxicity to the host. Several major obstacles stand in the way of developing novel antimicrobials by dimerization of existing antimicrobial agents. These obstacles include cell permeability problems, unexpected binding to additional cellular targets, reduction in target affinity due to the chemical modification of the parent antibiotics, and unexpected bacterial resistance.

A different approach for the design of novel ribosome-targeting antimicrobial agents is based on the design of hybrid antibacterials derived from fragments of ribosome targeting antibiotics.[22, 23] This should result in antibacterials that bind to rRNA with higher affinity, evade known modes of resistance, and more effectively cause bacterial cell death. Most bacterial ribosome-targeting antibiotics have a single binding site on the ribosome; therefore only one monomer unit of a designed antimicrobial homo-dimer can bind to the target at one time. However, homo-dimerization increases the local concentration of the drug and may therefore lead to improvement in target inhibition. Moreover, if an antimicrobial agent has more than one possible binding domain and these domains are in close proximity on the ribosome, homo-dimerization may result in improved target affinity. One such example was previously reported. Using surface plasmon resonance (SPR) experiments, it was demonstrated that the pseudo-disaccharide neamine (NEA, Figure 1), a segment of several common aminoglycoside (AG) antibiotics, bound to an rRNA sequence that is a model for the prokaryotic A-site in a 2:1 ratio, suggesting that AGs can bind to two sites that are in close proximity.[24] Based on these observations, NEA homo-dimers were designed and synthesized using various linkers. These homo-dimers had significantly increased affinity for the target A-site rRNA compared to the parent monomer and bound to the target in a 1:1 ratio. Furthermore, some NEA homo-dimers were poor substrates for AG-modifying enzymes (AMEs) that confer resistance to AGs through chemical modifications and demonstrated more potent antimicrobial activity than the parent monomer NEA. Finally, homo- and hetero-dimers[25–27] and oligomers[28] of known rRNA-targeting antibiotics have been explored for targeting viral RNAs or endogenous RNAs involved in disease in an attempt to inhibit their biological activity.

We are particularly interested in systematically exploring the potential that lies in the development of novel antimicrobial agents through the dimerization of intact structures of ribosome-targeting antibiotics. For that purpose, we designed and synthesized a complete combinatorial set of homo- and hetero-dimers composed of three different ribosome-targeting antibiotics and studied several aspects of their antimicrobial activity. The three antibiotics that served as starting materials were tobramycin (**1**), clindamycin (**2**), and

chloramphenicol (**3**). Each chosen antibiotic binds to a different site on the bacterial ribosome (Figure 1).

The AG **1**, which targets the A-site, is particularly effective for the treatment of infections caused by the pathogenic Gram-negative bacterium *Pseudomonas aeruginosa*.[29] Several mechanisms of resistance have evolved against **1**: reduction in the intracellular concentration of this antibiotic by efflux pump proteins or through reduced membrane permeability, structural modifications of the 16S rRNA leading to reduced target affinity, and deactivation by AMEs. AMEs are divided into three families: AG nucleotidyltransferases (ANTs), AG phosphotransferases (APHs), and AG acetyltransferases (AACs).[30] In addition to the increasing problem of antibiotic resistance, like other AGs, **1** causes reversible nephrotoxic and irreversible ototoxic side effects.[30]

A 2.54-Å resolution structure of a complex of an A-site 16S rRNA sequence and **1** revealed that the five amine groups of **1**, which are bound in their ammonium form, participate in hydrogen bonds with either bridging water molecules or directly with the target 16S rRNA nucleotides.[31] All of the alcohols of this AG, with the exception of its single C-6" primary alcohol, also interact with A-site nucleotides. We therefore chose to chemically modify the 6" primary alcohol of **1** to facilitate the attachment of the linker unit that was used for the preparation of the desired tobramycin-derived dimers.

The lincosamide antibiotic **2** is effective against staphylococci and streptococci infections.[32] Bacterial resistance to **2** occurs rarely through enzymatic deactivation and more prevalently as a result of 23S rRNA modifications, which reduce affinity of **2** for the ribosome and decrease its clinical efficacy.[33, 34] The structure of **2** bound to the 50S subunit of the *E. coli* ribosome indicated that the C-7 chloride atom does not specifically interact with the ribosomal RNA or proteins.[8] We therefore chose the C-7 of **2** as a suitable position for the attachment of a linker unit through nucleophilic displacement of the chloride atom leading to inversion of the absolute configuration of the C-7 position of **2**.

Finally, the antibiotic **3** is widely used against a broad spectrum of Gram-positive and Gram-negative bacteria including anaerobes.[35] Resistance to this antimicrobial agent occurs through reduced membrane permeability, mutation of the 50S ribosomal subunit, and deactivation by three different types of enzymes, chloramphenicol acetyltransferase (CAT), chloramphenicol phosphotransferase (CPT), and chloramphenicol nitroreductase (CNR).[36] Treatment with **3** may cause severe side effects such as aplastic anemia and bone marrow suppression, and there is a need for analogs of **3** that are safer for clinical use.[37] The antibiotic **3** binds specifically to nucleotides of the 23S rRNA and prevents peptide bond formation.[8, 10] X-ray crystallography of **3** bound to the 50S subunit of the *E. coli* ribosome revealed that the two chloride atoms of its dichloroacetamide segment appear to have no significant role in target binding. Therefore, we chose to modify this position of **3** for the generation of a linker attached monomer unit to be used for the generation of the desired dimeric structures.

RESULTS AND DISCUSSION

Synthesis of ribosome-targeting antibiotic dimers

Following the robust strategy for the synthesis of the homo- and hetero-dimers of AGs that was reported by Tor and co-workers,[27] we chose to attach a bis(2-mercaptoethyl) ether unit to each of the chosen ribosome-targeting antibiotics (Scheme 1). To prepare derivatives of **1**, compound **4** was reacted with bis(2-mercaptoethyl) ether to form compound **5** (Scheme 1A) as was previously reported.[27] Boc groups were removed by treatment with neat TFA to yield derivative **6**. Compound **5** was then reacted with 2,2'-dipyridyldisulfide to form the activated

disulfide derivative **7** that was used for the preparation of tobramycin-based disulfide-linked homo- and hetero-dimers.

The C-7 chloride of **2** served as a leaving group and was displaced by a bis(2-mercaptoethyl) ether unit to form the intermediate S_N2 product, which was per-acetylated to facilitate the isolation of the clindamycin analog **8** (Scheme 1B). Two different products were obtained depending on conditions used for the removal of acetyl groups of **8**. When 0.04 M of compound **8** was treated with an excess of sodium methoxide in MeOH and stirred at ambient temperature for 3 hours, the deprotected monomer **9** was obtained as the major product (83% isolated yield). However, when the reaction was ten-fold more concentrated (0.4 M of compound **8**), and **8** was treated overnight with an excess of sodium methoxide at ambient temperature, the disulfide linked clindamycin-derived homo-dimer **10** was obtained as the major product (75% isolated yield).

Compound **14** was obtained by preparing **12** from 2-amino-1-(4-nitrophenyl)-1,3-propanediol.[38] The α-chloride atom of **12** was displaced by bis(2-mercaptoethyl) ether to yield **13**. Reaction of **13** with 2,2'-dipyridyldisulfide yielded the activated disulfide **14** (Scheme 1C).

With the building block monomers in hand, we then prepared the rest of the five combinations of homo- and hetero-dimers (**16, 18, 22, 24** and **26**, Scheme 2) to form the complete set of six possible combinations of disulfide-linked dimers of the three chosen ribosome-targeting antibiotics. In the case of the tobramycin-containing dimers, all of the Boc protecting groups were readily removed by short treatment with neat TFA. The synthesis of homo-dimer **16** was previously reported; this dimeric AG was a significantly better inhibitor of the activity of the *Tetrahymena* ribozyme than the parent antibiotic **1**.[27]

To test the effect of linker length, we also prepared three dithioether-based dimers with short linkers. Nucleophilic displacement of the α-chloride atom of **12** by thiol **5** gave the hetero-dimer **19**, which was converted to **20**, the short linker analog of hetero-dimer **22**, by removal of the Boc groups. A similar strategy was used for synthesis of hetero-dimer **23** and for the preparation of homo-dimer **25**, the short linker analogs of hetero-dimers **24** and **26**, respectively.

Correlation between antimicrobial activity and *in vitro* inhibition of prokaryotic translation

We tested the antimicrobial potency of the synthetic antibiotic dimers against a selection of Gram-positive and Gram-negative pathogens (Table 1), and analyzed the relationship between their antimicrobial activities and protein translation inhibition properties by performing *in vitro* translation assays using extracts containing *E. coli* ribosomes (Table 2).

Compared to the parent antibiotic **1** (IC_{50} = 0.015 ± 0.001 μM), compound **6** was approximately 29-fold less potent as an inhibitor of *in vitro* translation (IC_{50} = 0.43 ± 0.01 μM); the corresponding homo-dimer **16** (IC_{50} = 0.27 ± 0.01 μM) was 18-fold less potent than **1**. Antimicrobial activities were strain dependent: In the case of *B. subtilis* 168 (strain A) and of *H. influenzae* ATCC 51907 (strain J), homo-dimer **16** was one to two double dilutions more potent than parent antibiotic **1** and two double dilutions more potent than the monomer building block **6** (Table 1). Monomer **6** and homo-dimer **16** were less potent than **1** against bacterial strains B, C, H, I, and K (Table 1). In general, the MIC values of compound **6** and of the homo-dimer **16** were similar in the majority of the tested strains. The fact that both compound **6** and homo-dimer **16** were poor inhibitors of *in vitro* translation compared to **1** but were potent against several of the tested bacterial strains suggests that the mode of action of these compounds may differ from that of the parent AG **1**.

Compared to the parent drug **2**, compound **9** proved a poor inhibitor of prokaryotic translation with IC_{50} values higher than 100 μM, at least 5-fold higher than that of the parent antibiotic **2**. In contrast to the monomer building block **9**, the homo-dimer **10** was about 3-fold more potent in the *in vitro* translation assay than the parent antibiotic **2** (IC_{50} values of 6.1 ± 1.1 μM and 18.1 ± 0.8 μM, respectively). Although compound **9** was a poor inhibitor of *in vitro* translation, it had MIC values of 1.2–9.4 μg/mL against seven of the tested strains, suggesting that the activity of this compound is not due to inhibition of prokaryotic translation. The dimer of **9**, homo-dimer **10**, was a considerably better inhibitor of *in vitro* translation than **2**. Homo-dimer **10** exhibited good antimicrobial activity against eight of the tested bacterial strains with MICs of 0.6–9.4 μg/mL. Moreover, compound **10** was significantly more active than its monomer building block **9** and comparable in activity to the parent antibiotic **2** against seven of the tested bacterial strains (B–G, K).

In the *in vitro* prokaryotic translation assay, the chloramphenicol-based monomer **13** was close to 8-fold less potent than the parent antibiotic **3** (Table 2). Compared to compound **13**, the chloramphenicol-based homo-dimers **25** and **26** exhibited a modest improvement in inhibition of prokaryotic translation (IC_{50} values 48.7 ± 1.8 μM for **13**, 32.9 ± 2.6 μM for **25**, and 25.6 ± 2.1 μM for **26**). Both the compounds **13** and **25** demonstrated poor antimicrobial activities compared to **3** against all of the tested bacterial strains. On the other hand, homo-dimer **26** was as potent as the parent against *L. monocytogenes* ATCC 19115 (strain E, MIC of 9.4 μg/mL) and was approximately 16-fold more potent than **3** against *S. aureus* ATCC 29213 (strain F).

Interestingly, the measured IC_{50} values of the inhibition of the *in vitro* prokaryotic translation of all hetero-dimers (**18, 20, 22, 23**, and **24**) were in the range bracketed by activities of the parent antibiotics from which these hetero-dimers were derived from (Table 2). For example, the IC_{50} value of the tobramycin-clindamycin hetero-dimer **18** in the *in vitro* translation assay was 0.98 ± 0.05 μM, which was approximately 65-fold higher than that of **1** and about 18-fold lower than that of **2**. The linker type and length had almost no effect on the inhibition of prokaryotic translation (Table 2, compare **25** and **26, 20** and **22**, as well as **23** and **24**). On the other hand, the linker type and length had a significant effect on the antimicrobial activity: The short linker homo- and hetero-dimers (**20, 23**, and **25**) were far less potent antimicrobial agents than the corresponding long disulfide linker hetero-dimers (**22, 24**, and **26**) against all of the tested strains (Table 1). The only exceptions were observed in the case of compounds **20** and **22**; the short linker hetero-dimer **20** was one double dilution more potent than the long disulfide linker hetero-dimer **22** against *S. epidermidis* ATCC 12228 (biofilm negative, strain K) and against *S. pyogenes* serotype M12 *str*. MGAS9429 (strain L).

To investigate the potential effect of active efflux on our compounds, we determined MIC values against *S. aureus* that expresses NorA (strain G), a protein that mediates the active efflux of hydrophilic drugs from the cells to confer resistance. We observed that this mechanism of resistance does not appear to affect molecules containing **1**- or **2**-based building blocks as the MIC values of compounds **10, 16**, and **18** were comparable to those of the parent drugs.

Effect of dimers on drug-modifying enzyme activity

To investigate the effect of covalently linking two intact ribosome-targeting antibiotics on the activity of drug-modifying enzymes responsible for the deactivation of the parent drugs in a wide spectrum of antibiotic-resistant bacterial strains, we selected six AMEs and three chloramphenicol-modifying enzymes against which we tested all tobramycin- and chloramphenicol-derived homo- and hetero-dimers (Figure 2).

The substrate preference of the nine tested drug-deactivating enzymes varied. Of the six tested tobramycin-targeting AMEs, the acetyltransferase activity of the bifunctional AAC(6')/APH(2''), the acetyltransferase activity of AAC(6')-Ib', and the nucelotidyltransferase activity of ANT(4') were significantly less against tobramycin-derived dimers **16, 18, 22**, and **20** than against the parent AG **1** (Figure 2A and Table S1). The activity of all AMEs was set to 100% for the parent antibiotic **1** for comparison purposes. Dimers **16, 18, 22** and **20** were poor substrates of AAC(6')-Ib' (39%, 20%, 31%, and 37%, respectively). The tobramycin derivatives **16, 18**, and **22** were also poorer substrates of AAC(6')/APH(2'') (34%, 31%, and 34%, respectively). Moreover, tobramycin-derived dimers **18** and **22** were poorer substrates of ANT(4') (38% and 28%, respectively) than **16** and **20** (90% and 63%, respectively). Tobramycin derivative **6**, with the thiol-containing linker, could only be tested against ANT(4') as our assay for AAC enzymes relies on detection of free thiol. Compound **6** was a poorer substrate of ANT(4') (49%) than the parent AG **1** (100%). The opposite effect was observed for the other three AMEs tested; compared to the parent AG **1**, all of the tobramycin-based dimers (**16, 18, 20** and **22**) were superior substrates for the acetyltransferases AAC(3)-IV, AAC(2')-Ic, and Eis (Figure 2A). Overall, compounds **18** and **22** behaved similarly with all AMEs and were poorer substrates then **16** and **20**. With AAC(3)-IV, AAC(2')-Ic, and Eis, compounds **18** and **22** were 1.4-, 1.6-, and ~2.6-fold better substrates, respectively than **1**, whereas compound **16** was a 2-, 2.4-, and 4.1-fold better substrate than **1**, and compound **20** was 1.8-, 2.0-, and 2.9-fold better than **1**.

The chloramphenicol-derived homo-dimer **25** was a poor substrate for all of the three chloramphenicol-modifying enzymes: CPT, CNR, and CAT_I (Figure 2B and Table S1). However, this homo-dimer demonstrated poor antimicrobial activity against all bacterial strains tested (Table 1). With the exception of homo-dimer **25**, CNR readily modified all chloramphenicol-derived dimers (**20**, 76%; **22**, 117%; **23**, 133%; **24**, 174%; and **26**, 220%) at least as well as it modified the parent antibiotic **3** (100%) (Figure 2B). The chloramphenicol acetyltransferase CAT_I is commonly found in chloramphenicol-resistant bacteria. Of the tested chloramphenicol-modifying enzymes, all of the chloramphenicol-derived dimers (**20**, 82%; **22**, 70%; **23**, 10%; **24**, 69%; and **26**, 73%) were poorer substrates of CAT_I than the parent antibiotic **3** (100%). With the CPT, all chloramphenicol-derived dimers behaved similarly to **3**, with relative activities ranging from 91–139%. With the exception of dimers **25** and **26**, the length and type of the linker did not significantly affect the resistance profile of the dimers. The dimer approach proved to be more effective in interfering with the drug-modifying activities of the tested AMEs than with the activities of the three tested chloramphenicol-modifying enzymes.

CONCLUSION

In this study we describe the synthesis of nine homo and hetero-dimers composed of combinations of the three intact structures of the bacterial ribosome-targeting antibiotics **1–3**. The effect of the homo- and hetero-dimerization approach was evaluated by testing the antimicrobial activity, the potency of the dimers as inhibitors of *in vitro* prokaryotic translation, and the ability of nine different drug-deactivating enzymes to modify the dimers derived from chloramphenicol and/or tobramycin.

Of the nine dimeric structures that were evaluated in this study, two homo-dimers exhibited potent antibacterial activities, which were in some cases superior to those of the parent antibiotics from which they were derived. Both the tobramycin-derived homo-dimer **16** and the clindamycin-derived homo-dimer **10** were comparable and in some cases more potent antimicrobials than the parents **1** and **2** against some of the twelve bacterial strains in our tested panel. The results of the *in vitro* inhibition of prokaryotic translation assay suggest

that **1** and the tobramycin-derived homo-dimer **16** may act through different modes of action. On the other hand, the clindamycin-derived homo-dimer **10** was approximately 3-fold more potent than the parent **2** as an inhibitor of prokaryotic translation. These results demonstrate that homo-dimerization of intact ribosome targeting antibiotics may lead to a change in the mode of action or to improved target inhibition.

Of the five hetero-dimers, compound **18** demonstrated a broader antimicrobial activity spectrum than either of the parent antibiotics. As was the case for several of the hetero-dimers, the *in vitro* inhibition of prokaryotic translation potency of compound **18** was between that of its parent antibiotics **1** and **2**.

The effect of drug-modifying enzymes on the dimers depended on the enzyme. Some drug-deactivating enzymes modified dimers more efficiently than they did the parent antibiotics. On the other hand, the two potent tobramycin-derived compounds **16** and **18** were approximately 2.5–5 times less prone to deactivation by the two AG-modifying enzymes AAC(6')/APH(2'') and AAC(6')-Ib' than was the parent AG **1**. AAC(6') enzymes account for high levels of AG resistance and are prevalently found amongst AG-resistant bacterial strains. Hence both homo- and hetero-dimerization of ribosome-targeting antibiotics can be used to combat certain AG resistance mechanisms. This study demonstrates that even though the diversity amongst bacterial pathogens makes it impossible to predict all of the possible effects of drug dimerization, dimerization is a promising strategy for development of novel inhibitors of bacterial protein translation. Further exploration of this strategy should result in novel antimicrobial agents that may bind to the prokaryotic ribosome through unique sets of interactions that differ from those of the parent antibiotics.

EXPERIMENTAL SECTION

Bacterial strains, plasmids, materials, and instrumentation

The bacterial strains tested in this study were obtained from a variety of sources. *Bacillus subtilis* 168 (A) was obtained from the Bacillus Genetic Stock Center (Columbus, OH, USA). *Bacillus subtilis* 168 with AAC(6')/APH(2'')-pRB374 (B) was prepared as we previously described.[39] *Mycobacterium smegmatis* str. MC2 155 (C) was a generous gift from Dr. Sabine Ehrt (Weill Cornell Medical College). *Bacillus cereus* ATCC 11778 (D), *Listeria monocytogenes* ATCC 19115 (E), *Staphylococcus aureus* ATCC 29213 (F), and *Escherichia coli* MC1061 (H) were provided by Prof. Paul J. Hergenrother (University of Illinois at Urbana-Champaign). *Staphylococcus aureus* NorA (G) was a gift from Prof. David Sherman (University of Michigan). *Bacillus anthracis* 34F2 Sterne strain (I) was a gift from Prof. Philip C. Hanna (University of Michigan). *Haemophilus influenzae* ATCC 51907 (J) and *Staphylococcus epidermidis* ATCC 12228 (biofilm negative) (K) were purchased from ATCC. *Streptococcus pyogenes* M12 *str*. MGAS9429 (L) was provided by Prof. Doron Steinberg (The Hebrew University of Jerusalem). Chemically competent *E. coli* TOP10 and BL21 (DE3) used in cloning were purchased from Invitrogen. The Int-pET19b–pps plasmid was a gift from Dr. Tapan Biswas (University of Michigan). All restriction enzymes, T4 DNA ligase, and Phusion DNA polymerase were purchased from NEB. DNA primers for PCR were purchased from Integrated DNA Technologies. DNA sequencing was performed at the University of Michigan Sequencing Core. Chemical reagents used in enzymatic assays, NADH, DTNB, AcCoA, ATP, phosphoenol pyruvate (PEP), lactic dehydrogenase (LDH) and pyruvate kinase (PK) were purchased from Sigma-Aldrich. The pH was adjusted at room temperature. Spectrophotometric assays were performed on a multimode SpectraMax M5 plate reader using 96-well plates. The Wizard Genomic DNA purification kit (catalog #A1120) used for isolation of *H. influenzae* ATCC 51907 genomic DNA was purchased from Promega (Madison, WI). The pET16b plasmid containing the CPT gene[40] used as a template for the cloning of the pCPT-Int-pET19b–pps was provided

by Dr. Jacqueline Ellis (University of Leicester). Chemical reactions were monitored by TLC (Merck, Silica gel 60 F_{254}) and visualized using a cerium-molybdate stain ($(NH_4)_2Ce(NO_3)_6$ (5 g), $(NH_4)_6Mo_7O_{24}•4H_2O$ (120 g), H_2SO_4 (80 mL), H_2O (720 mL)). Compounds were purified by SiO_2 flash chromatography (Merck Kieselgel 60). ^1H (including 1D-TOCSY) and ^{13}C NMR spectra were recorded on Bruker Avance™ 400 and 500 spectrometers (Figs. S1–S30). Low-resolution electrospray ionization (LRMS (ESI)) mass spectra were recorded on a Waters 3100 mass detector. High-resolution electrospray (ESI-MS) mass spectra were recorded on a Waters Synapt instrument. The purity of the new dimers was determined by reversed-phase high-performance liquid chromatography (RP-HPLC, C18 column, 5 μ, 250×4.6 mm) using a gradient of 1:9 to 9:1 acetonitrile:H_2O (0.1% TFA) over 30 min at 1 mL/min (Table S2 and Figs. S31– S39) and the identity of the compound was confirmed by mass spectrometry. The purity of all of the dimers tested was ≥95%.

Compound 6

Compound **6** was synthesized as previously reported.[27] ^1H NMR (500 MHz, D_2O) δ 5.67 (d, J = 3.6 Hz, 1H, H-1'), 5.01 (d, J = 3.7 Hz, 1H, H-1''), 3.98-3.90 (m, 2H, H-4, H-5''), 3.87 (m, 2H, H-2'', H-5'), 3.83-3.72 (m, 3H, H-5, H-4', H-6), 3.72-3.57 (m, 7H, H-4', H-4'', H-2', $SCH_2CH_2OCH_2CH_2S$ (4H)), 3.51 (m, 2H, H-1, H-3), 3.42-3.31 (m, 2H, H-3'', H-6'), 3.19 (m, 1H, H-6'), 3.02 (ddd, J_1 = 14.1 Hz, J_2 = 6.7 Hz, J_3 = 2.6 Hz, 1H, H-6''), 2.88 (m, 2H, $SCH_2CH_2OCH_2CH_2S$), 2.82-2.71 (m, 3H, $SCH_2CH_2OCH_2CH_2S$ (2H), H-6''), 2.48 (dt, J_1 = 12.7 Hz, J_2 = 4.3 Hz, 1H, H-2eq), 2.23 (dt, J_1 = 12.1 Hz, J_2 = 4.4 Hz, 1H, H-3eq), 1.95 (q, J = 12.3 Hz, 1H, H-3ax), 1.87 (q, J = 12.6 Hz, 1H, H-2ax) (Fig. S1). ^{13}C NMR (125 MHz, D_2O) δ 163.0 (q, J = 35.3 Hz, $CF_3\underline{C}O_2H$), 116.3 (q, J = 291.6 Hz, $\underline{C}F_3CO_2H$), 100.7, 94.5, 83.8, 77.6, 74.2, 72.6, 71.8, 69.0, 68.0 (2C), 64.4, 54.6, 49.5, 48.4, 47.8, 39.8, 32.7, 31.9, 29.9 (2C), 29.3, 27.8, 23.1 (Fig. S2). HRMS (ESI) *m/z* calcd for $C_{22}H_{45}N_5O_9S_2$ $[M+H]^+$ 588.2737, found 588.2741.

Compound 8

Bis(2-mercaptoethyl)ether (3.76 mL, 30.35 mmol) was added to a solution of clindamycin hydrochloride (2 g, 4.33 mmol) and Cs_2CO_3 (2.8 g, 8.60 mmol) in DMF (6 mL). The reaction mixture was stirred at 50 °C for 12 h. The reaction progress was monitored by ESI MS by following the disappearance of the starting material ($[M+H]^+$, *m/z* 425.50) and the formation of **8** ($[M+H]^+$, *m/z* 527.58). Upon completion, the reaction mixture was diluted with EtOAc and washed with 0.1 M HCl and brine. The organic layer was dried over $MgSO_4$ and concentrated under reduced pressure. Purification by flash column chromatography (SiO_2, 0.5:99.5 to 3:97/MeOH:CH_2Cl_2) afforded a mixture of the desired product and traces of a byproduct that could only be separated from the desired product after the acetylation reaction (1.7 g, 74%). The mixture (1.4 g, 2.6 mmol) was dissolved in anhydrous pyridine (4 mL). Ac_2O (2 mL, 21.3 mmol) and a catalytic amount of DMAP were added and the mixture was stirred at rt. The reaction progress was monitored by TLC (9:1/ EtOAc:hexane). After 2 h, the reaction mixture was neutralized by adding 1 N HCl and partitioned between H_2O and EtOAc. The organic layer was washed with brine, dried over $MgSO_4$, and concentrated under reduced pressure. Purification by flash column chromatography (SiO_2, 1:99 to 4:96/MeOH:CH_2Cl_2) afforded **8** (1.60 g, 87%) as a white solid. ^1H NMR (400 MHz, CD_3OD) δ 5.67 (d, J = 5.7 Hz, 1H, H-4), 5.30 (d, J = 3.2 Hz, 1H, H-1), 5.23 (dd, J_1 = 11.0 Hz, J_2 = 5.7 Hz, 1H, H-3), 5.11 (dd, J_1 = 11.0 Hz, J_2 = 3.3 Hz, 1H, H-2), 4.64-4.38 (m, 2H, H-5, H-6), 3.77-3.63 (m, 2H, $SCH_2CH_2OCH_2CH_2SAc$), 3.61-3.58 (m, 2H, $SCH_2CH_2OCH_2CH_2SAc$), 3.44 (qt, J_1 = 7.0 Hz, J_2 = 2.1 Hz, 1H, H-7), 3.25 (dd, J_1 = 8.0, J_2 = 6.0 Hz, 1H, H-2'), 3.05-3.16 (m, 2H, $SCH_2CH_2OCH_2CH_2SAc$), 2.90 (dd, J_1 = 3.8 Hz, J_2 = 1.0 Hz, 1H, H-3'), 2.89-2.81 (m, 1H, $SCH_2CH_2OCH_2CH_2SAc$), 2.63 (dt, J_1 = 12.6 Hz, J_2 = 6.2 Hz, 1H, $SCH_2CH_2OCH_2CH_2SAc$), 2.42 (s, 3H, $NC\underline{H}_3$), 2.36 (s, 3H,

$SC\underline{H}_3$), 2.17 (s, 3H, $C(=O)C\underline{H}_3$), 2.13 (s, 3H, $C(=O)C\underline{H}_3$), 1.95 (s, 3H, $C(=O)C\underline{H}_3$), 1.97-2.03 (m, 3H, H-5'a, H-5'b, and H-3'),1.94 (s, 1H, $C(=O)C\underline{H}_3$), 1.14 (m, 1H, H-4'), 1.78-1.26 (m, 4H, H-1" (2H), H-2" (2H)), 1.21 (d, J = 7.1 Hz, 3H, H-8), 0.94 (t, J = 6.8 Hz, 3H, H-3") (Fig. S3). ^{13}C NMR (100 MHz, CD_3OD) δ 197.1, 177.3, 172.0, 171.6 (2C), 86.0, 72.2, 70.5, 70.1, 69.8, 69.2, 68.9, 68.7, 63.9, 42.1, 41.3, 38.9, 38.1, 36.9, 31.2, 30.5, 29.7, 22.4, 21.0, 20.6 (2C), 14.6 (2C), 13.8 (Fig. S4). LRMS (ESI) *m/z* cald for $C_{30}H_{51}N_2O_{10}S_3$ $[M+H]^+$ 695.26, found 695.56.

Compound 9

Sodium methoxide (200 μL of 0.5 M solution in MeOH) was added in four portions of 50 μL to a solution of **8** (160 mg, 0.23 mmol) in MeOH (5 mL). The reaction progress was monitored by TLC (1:9/MeOH:CH_2Cl_2). After 3 h, the excess sodium methoxide was quenched with a few drops of glacial AcOH. The solvent was evaporated and the residue purified by flash chromatography (SiO_2, 1:99 to 6:94/MeOH:CH_2Cl_2) to afford **9** (100 mg, 83%) as a white powder. ^{1}H NMR (400 MHz, CD_3OD) δ 5.28 (d, J = 5.6 Hz, 1H, H-1), 4.46 (dd, J_1 = 9.6 Hz, J_2 = 3.8 Hz, 1H, H-6), 4.17 (dd, J_1 = 9.9 Hz, J_2 = 1.1 Hz, 1H, H-5), 4.13 (dd, J_1 = 10.2 Hz, J_2 = 5.6 Hz, 1H, H-2), 3.8 (dd, J_1 = 3.3 Hz, J_2 = 1.1 Hz, 1H, H-4), 3.69-3.63 (m, 2H, $SCH_2CH_2OCH_2CH_2S$), 3.62-3.58 (m, 2H, $SCH_2CH_2OCH_2CH_2S$), 3.56 (dd, J_1 = 3.3 Hz, J_2 = 1.1 Hz, 1H, H-3), 3.45 (qd, J_1 = 7.0 Hz, J_2 = 3.7 Hz, 1H, H-7), 3.25 (dd, J_1 = 8.6 Hz, J_2 = 6.0 Hz, 1H, H-3'), 3.01 (dd, J_1 = 10.5 Hz, J_2 = 5.0 Hz, 1H, H-2'), 2.85 (dt, J_1 = 13.8 Hz, J_2 = 6.3 Hz, 1H, $SCH_2CH_2OCH_2CH_2S$), 2.78-2.62 (m, 3H, $SCH_2CH_2OCH_2CH_2SH$), 2.45 (s, 3H, $NC\underline{H}_3$), 2.29-2.00 (m, 3H, H-5' (2H), H-3'), 2.15 (s, 3H, $SC\underline{H}_3$), 1.87 (ddd, J_1 = 13.0 Hz, J_2 = 10.5 Hz, J_3 = 9.4 Hz, 1H, H-4'), 1.40 (m, 4H, H-1" (2H), H-2" (2H)), 1.31 (d, J = 7.5 Hz, 3H, H-8), 0.94 (m, 3H, H-3") (Fig. S5). ^{13}C NMR (100 MHz, CD_3OD) δ 176.9, 88.9, 72.4, 70.6 (2C), 69.4, 69.0, 68.6, 68.1, 62.4, 50.4, 40.6, 39.8, 37.5, 37.3, 35.7, 29.9, 23.4, 21.2, 14.0, 13.2, 12.7 (Fig. S6). HRMS (ESI) *m/z* calcd for $C_{22}H_{42}N_2O_7S_3$ $[M+H]^+$ 527.2283, found 527.2280.

Compound 10

Sodium methoxide (200 μL of 0.5 M solution in MeOH) was added to a solution of **8** (40 mg, 0.12 mmol) in MeOH (0.15 mL). The reaction progress was monitored by TLC (1:9/ MeOH:CH_2Cl_2). When **10** was the major product observed by TLC, a few drops of glacial AcOH were added to the reaction mixture, the solvent was evaporated, and the residue purified by flash chromatography (SiO_2, 1:99 to 10:90/MeOH:CH_2Cl_2) to afford **10** (46 mg, 75%) as a white powder. Purity = 97% (Table S2 and Fig. S31). ^{1}H NMR (400 MHz, CD_3OD) δ 5.29 (d, J = 5.7 Hz, 2H, H-1), 4.44 (dd, J_1 = 9.5 Hz, J_2 = 3.8 Hz, 2H, H-6), 4.17 (d, J = 9.6 Hz, 1.1 Hz, 2H, H-5), 4.13 (dd, J_1 = 10.2 Hz, J_2 = 5.6 Hz, 2H, H-2), 3.80 (dd, J_1 = 3.3 Hz, J_2 = 1.1 Hz, 2H, H-4), 3.75 (t, J = 6.3 Hz, 4H, $SCH_2CH_2OCH_2CH_2S$), 3.70-3.65 (m, 4H, $SCH_2CH_2OCH_2CH_2S$), 3.57 (dd, J_1 = 10.2 Hz, J_2 = 3.4 Hz, 2H, H-3), 3.43 (dd, J_1 = 7.1 Hz, J_2 = 3.9 Hz, 2H, H-7), 3.25 (dd, J_1 = 8.6 Hz, J_2 = 6.0 Hz, 2H, H-5'), 3.00 (dd, J_1 = 10.5 Hz, J_2 = 5.0 Hz, 2H, H-2'), 2.94 (t, J = 6.3 Hz, 4H, $SCH_2CH_2OCH_2CH_2S$), 2.84 (dt, J_1 = 13.6 Hz, J_2 = 6.5 Hz, 4H, $SCH_2CH_2OCH_2CH_2S$), 2.72 (dt, J_1 = 13.6 Hz, J_2 = 6.5 Hz, 2H, $SCH_2CH_2OCH_2CH_2S$), 2.45 (s, 3H, $NC\underline{H}_3$), 2.29-2.18 (m, 2H, H-5'), 2.16 (s, 6H, $SC\underline{H}_3$), 2.07-1.97 (m, 4H, H-3'), 1.86 (ddd, J_1 = 12.9 Hz, J_2 = 10.5 Hz, J_3 = 9.3 Hz, 2H, H-4'), 1.36 (m, 8H, H-1" (4H), H-2" (4H)), 1.28 (d, J = 7.1 Hz, 6H, H-8), 0.95 (m, 6H, H-3") (Fig. S7). ^{13}C NMR (100 MHz, CD_3OD) δ 178.4 (2C), 90.3 (2C), 72.1 (4C), 70.8 (2C), 70.5 (2C), 70.1 (2C), 70.0 (2C), 69.5 (2C), 63.9 (2C), 52.0 (2C), 42.1 (2C), 41.2 (2C), 39.7 (2C), 38.9 (2C), 38.7 (2C), 37.1 (2C), 31.3 (2C), 22.6 (2C), 15.5 (2C), 14.6 (2C), 14.1 (2C) (Fig. S8). HRMS (ESI) *m/z* calcd for $C_{44}H_{82}N_4O_{12}S_6$ $[M+H]^+$ 1051.4332, found 1051.4320.

Compound 12

This compound was prepared using a modified version of a previously published procedure.[38] *N*,*N*-Diisopropylethylamine (8 mL, 0.045 mol) was added to 2-amino-1-(4-nitrophenyl)-1,3-propanediol (4 gr, 0.18 mole) dissolved in MeOH (40 mL). The mixture was cooled in an ice bath and chloroacetyl chloride (3 mL, 0.036 mol) was added. The reaction progress was monitored by TLC (1:9/MeOH:CH_2Cl_2). After 5 h, when **12** was observed as the major product, the reaction mixture was partitioned between H_2O and EtOAc. The aqueous layer was separated and extracted with EtOAc. The combined organic layers were washed with brine, dried over $MgSO_4$, and concentrated under reduced pressure. Purification by flash chromatography (SiO_2, 1:99 to 4:96/MeOH:CH_2Cl_2) afforded **12** (3.6 g, 67%) as a white solid. ^{1}H NMR (400 MHz, CD_3OD) δ 8.14 (d, *J* = 8.6 Hz, 2H, H-1), 7.63 (d, *J* = 8.6 Hz, 1H, H-2), 5.17 (d, *J* = 2.9 Hz, 1H, H-3), 4.21 (dt, J_1 = 6.7 Hz, J_2 = 3.4 Hz, 1H, H-4), 4.0 (d, *J* = 14.0 Hz, 2H, H-6), 3.96 (d, *J* = 14.0 Hz, 2H, H-6) 3.81 (dd, J_1 = 11.1 Hz, J_2 = 6.6 Hz, 1H, H-5), 3.64 (dd, J_1 = 11.1 Hz, J_2 = 6.1 Hz, H-5) (Fig. S9). ^{13}C NMR (100 MHz, CD_3OD) δ 169.1, 151.0, 148.1, 128.1 (2C), 124.1 (2C), 71.4, 62.1, 57.8, 43.1 (Fig. S10). LRMS (ESI) *m/z* cald for $C_{11}H_{12}ClN_2O_5$ $[M-H]^-$ 287.05, found 287.28.

Compound 13

Bis(2-mercaptoethyl)ether (0.85 mL, 6.94 mmol) and a catalytic amount of TBAI were added to a solution of **12** (1.00 g, 3.47 mmol) and K_2CO_3 (1.13 g, 3.47 mmol) in anhydrous THF (7 mL). The reaction mixture was stirred at 50 °C. The reaction progress was monitored by TLC (99:1/EtOAc:MeOH). After 3 h, the reaction mixture was partitioned between H_2O and EtOAc. The organic layer was washed with brine, dried over $MgSO_4$, and concentrated under reduced pressure. Purification by flash chromatography (SiO_2, 6:4/ petroleum ether:EtOAc to 99:1/EtOAc:MeOH) afforded **13** (1.35 g, quant.) as a white solid. ^{1}H NMR (400 MHz, CD_3OD) δ 8.22 (d, *J* = 8.7 Hz, 2H, H-1), 7.69 (d, *J* = 8.7 Hz, 2H, H-2), 5.17 (d, *J* = 2.6 Hz, 1H, H-3), 4.20 (ddd, J_1 = 7.3 Hz, J_2 = 5.9 Hz, J_3 = 2.7 Hz, 1H, H-4), 3.80 (dd, J_1 = 10.8 Hz, J_2 = 7.3 Hz, 1H, H-5), 3.62 (dd, J_1 = 10.8 Hz, J_2 = 5.9 Hz, 1H, H-5), 3.57 (dt, J_1 = 11.7 Hz, J_2 = 6.3 Hz, 4H, $SCH_2CH_2OCH_2CH_2S$), 3.23 (d, *J* = 14.9 Hz, 1H, H-6), 3.18 (d, *J* = 14.9 Hz, 1H, H-6), 2.66 (t, *J* = 6.4 Hz, 2H, $SCH_2CH_2OCH_2CH_2S$), 2.55 (t, *J* = 6.3 Hz, 2H, $SCH_2CH_2OCH_2CH_2S$) (Fig. S11). ^{13}C NMR (100 MHz, CD_3OD) δ 172.2, 152.0, 148.5, 128.3 (2C), 124.2 (2C), 73.8, 71.6, 71.3, 62.5, 58.0, 36.4, 32.8, 24.7 (Fig. S12). HRMS (ESI) *m/z* calcd for $C_{15}H_{22}N_2O_6S_2$ $[M+Na]^+$ 413.0817, found 413.0813.

Compound 14

2,2'-Dipyridyldisulfide (140 mg, 0.64 mmol) was added to a solution of compound **13** (125 mg, 0.32 mmol) in MeOH (4 mL), and the reaction mixture was stirred at 23 °C. The reaction progress was monitored by TLC (96:4/EtOAc:MeOH). After 5 h, the solvent was removed under reduced pressure. Purification by flash chromatography (SiO_2, 6:4/petroleum ether:EtOAc to 96:4/EtOAc:MeOH) afforded **14** (125 mg, 78%) as a white solid. ^{1}H NMR (400 MHz, CD_3OD) δ 8.40 (ddd, J_1 = 4.9 Hz, J_2 = 1.7 Hz, J_3 = 0.9 Hz, 1H, H-1'), 8.19 (d, *J* = 8.8 Hz, 2H, H-1), 7.93 (dd, J_1 = 8.1 Hz, J_2 = 1.2 Hz, 1H, H-3'), 7.83 (ddd, J_1 = 8.04 Hz, J_2 = 4.9 Hz, J_3 = 1.7, Hz, 1H, H-2'), 7.68 (d, *J* = 8.8 Hz, 2H, H-2), 7.23 (ddd, J_1 = 7.4 Hz, J_2 = 4.9 Hz, J_3 = 1.1 Hz, 1H, H-4'), 5.18 (d, *J* = 2.6 Hz, 1H, H-3), 4.21 (ddd, J_1 = 7.4 Hz, J_2 = 5.8 Hz, J_3 = 2.7 Hz, 1H, H-4), 3.80 (dd, J_1 = 10.8 Hz, J_2 = 7.3 Hz, 1H, H-5), 3.65 (m, 3H, H-5, $SCH_2CH_2OCH_2CH_2S$ (2H)), 3.51 (t, *J* = 6.3 Hz, 2H, $SCH_2CH_2OCH_2CH_2S$), 3.23 (d, *J* = 14.9 Hz, 1H, H-6), 3.18 (d, *J* = 14.9, 1H, H-6), 3.03 (t, *J* = 6.0 Hz, 2H, $SCH_2CH_2OCH_2CH_2S$), 2.52 (t, *J* = 6.4 Hz, 2H, $SCH_2CH_2OCH_2CH_2S$) (Fig. S13). ^{13}C NMR (100 MHz, CD_3OD) δ 172.2, 161.7, 152.0, 150.2, 148.5, 139.2, 128.3 (2C), 124.2 (2C), 122.3, 121.2, 71.6, 71.3, 69.5, 62.5, 58.0, 39.9, 36.5, 32.7 (Fig. S14). LRMS (ESI) *m/z* calcd for $C_{20}H_{25}N_3O_6S_3Cl$ $[M+Cl]^-$ 534.06, found 534.17.

Compound 16

Compound **16** was synthesized as previously reported.[27] Purity = 97% (Table S2 and Fig. S32). ^{1}H NMR (400 MHz, CD_3OD) δ 5.79 (d, *J* = 3.7 Hz, 2H, H-1'), 5.08 (d, *J* = 3.7 Hz, 4H, H-1"), 4.13 (t, *J* = 9.6 Hz, 2H, H-4), 3.99 (m, 4H, H-5', H-5"), 3.94-3.89 (m, 4H, H-2", H-5), 3.82-3.73 (m, 6H, H-5, $SCH_2CH_2OCH_2CH_2S$ (4H)), 3.69 (t, *J* = 6.4 Hz, 4H, $SCH_2CH_2OCH_2CH_2S$), 3.58 (m, 10H, H-1, H-3, H-2', H-4', H-4"), 3.46-3.37 (m, 4H, H-6', H-3"), 3.21-3.07 (m, 4H, H-6', H-6"), 2.91 (t, *J* = 6.3 Hz, 4H, $SCH_2CH_2OCH_2CH_2S$), 2.87-2.79 (m, 6H, $SCH_2CH_2OCH_2CH_2S$ (4H), H-6"), 2.57 (dt, J_1 = 12.5 Hz, J_2 = 4.3 Hz, 2H, H-2eq), 2.23 (dt, J_1 = 12.0 Hz, J_2 = 4.5 Hz, 2H, H-3eq), 2.19-2.04 (m, 4H, H-3ax, H-3eq) (Fig. S15). ^{13}C NMR (125 MHz, D_2O) δ 162.5 (q, *J* = 36.2 Hz, CF_3CO_2H), 116.0 (q, *J* = 290.9 Hz, CF_3CO_2H), 100.6 (2C), 94.3 (2C), 83.8 (2C), 77.4 (2C), 74.2 (2C), 72.5 (2C), 70.3 (2C), 69.1 (2C), 67.9 (4C), 64.4 (2C), 54.6 (2C), 49.5 (2C), 48.2 (2C), 47.8 (2C), 39.8 (2C), 37.0 (2C), 32.6 (2C), 31.8 (2C), 29.5 (2C), 29.2 (2C), 27.7 (2C) (Fig. S16). HRMS (ESI) *m/z* calcd for $C_{44}H_{88}N_{10}O_{18}S_4$ $[M+H]^+$ 1173.5239, found 1173.5245.

Compound 17

A solution of **7** (127 mg, 0.106 mmol) in MeOH (1 mL) was added to a solution of **9** (50 mg, 0.095 mmol) in MeOH (1 mL), and the reaction was stirred at 23 °C. The reaction progress was monitored by TLC (9:1/CH_2Cl_2:MeOH). Upon completion, the solvent was removed under reduced pressure. Purification by flash chromatography (SiO_2, 99:1 to 91:9/ CH_2Cl_2:MeOH) afforded **17** (135 mg, 88%) as a white solid. ^{1}H NMR (400 MHz, CD_3OD) δ 5.27 (d, *J* = 5.6 Hz, 1H, H-7), 5.13 (bs, 1H, H-1'), 5.06 (d, *J* = 3.7 Hz, 1H, H-1"), 4.42 (ddd, J_1 = 9.7 Hz, J_2 = 4.0 Hz, J_3 = 1.5 Hz, 1H, H-12), 4.16-4.08 (m, 2H, H-8, H-11), 3.78-3.71 (m, 8H, H-4, H-5', H-2", H-5", $SCH_2CH_2OCH_2CH_2S$ (4H)), 3.68-3.61 (m, 7H, H-5, H-6, H-10, $SCH_2CH_2OCH_2CH_2S$ (4H)), 3.58-3.33 (m, 10H, H-1, H-3, H-2', H-4', H-6', H-3", H-4", H-9, H-13, H-21), 3.23 (dd, J_1 = 8.6 Hz, J_2 = 5.8 Hz, 1H, H-6'), 3.06-3.02 (m, 1H, H-6"), 2.99 (dd, J_1 = 10.5 Hz, J_2 = 4.9 Hz, 1H, H-15), 2.93-2.89 (m, 4H, $SCH_2CH_2OCH_2CH_2S$), 2.85-2.87 (m, 4H, $SCH_2CH_2OCH_2CH_2S$), 2.75-2.65 (m, 1H, H-6"), 2.43 (s, 3H, $NC\underline{H}_3$), 2.25-1.94 (m, 7H, H-16 (2H), H-21, H-2eq, $SC\underline{H}_3$), 1.90-1.80 (m, 1H, H-3eq), 1.68-1.55 (m, 2H, H-2ax, H-3ax), 1.54-1.27 (m, 50H, H-17, $5xCO_2C(CH_3)_3$, H-18 (2H), H-19 (2H)), 1.35 (d, *J* = 7.0 Hz, 3H, H-14), 1.34 (q, *J* = 2.4 Hz, 3H), 0.92 (m, 3H, H-20). ^{13}C NMR (100 MHz, CD_3OD) δ 176.9, 158.0, 157.8, 156.5, 156.3, 148.7, 98.47, 97.99, 88.9, 82.5, 80.9, 79.3, 79.1, 79.0, 78.8, 72.6, 72.1, 70.6, 70.3, 69.4, 69.0, 68.7, 68.5, 68.1, 55.6, 50.5, 50.1, 49.6, 49.6, 40.7, 39.8, 39.8, 38.2, 38.2, 37.5, 37.3, 35.6, 34.4, 33.7, 32.9, 32.1, 29.8 (15C), 21.2, 14.1, 13.2, 12.7. LRMS (ESI) *m/z* calcd for $C_{69}H_{126}N_7O_{25}S_5$ $[M+H]^+$ 1612.73, found 1613.10.

Compound 18

Neat TFA (0.7 mL) was added to compound **17** (30 mg, 0.018 mmol) at rt. After 3 min, the TFA was removed under reduced pressure, and the product was re-dissolved in a minimal volume of H_2O and freeze-dried to afford **18** (32 mg, quant.) as a white foam. Purity = 96% (Table S2 and Fig. S33). ^{1}H NMR (500 MHz, D_2O) δ 5.67 (d, *J* = 3.6 Hz, 1H, H-1'), 5.28 (d, *J* = 5.9 Hz, 1H, H-7), 5.01 (d, *J* = 3.5 Hz, 1H, H-1"), 4.51 (dd, J_1 = 8.2 Hz, J_2 = 1.9 Hz, 1H, H-12), 4.22 (dt, J_1 = 8.0 Hz, J_2 = 3.6 Hz, 1H, H-11), 4.13 (m, 1H, H-8), 4.08-3.99 (m, 2H, H-4, H-5"), 3.95-3.70 (m, 16H, H-2", H-5', H-5, H-10, H-6, H-4', H-4", H-2', $SCH_2CH_2OCH_2CH_2S$ (8H)), 3.55-2.98 (m, 4H, H-1, H-3, H-9, H-13), 3.40-3.32 (m, 3H, H-3", H-6', H-21), 3.18 (m, 1H, H-6'), 3.02 (m, 1H, H-6"), 2.96 (m, 1H, H-15), 2.87 (s, 3H, $NC\underline{H}_3$), 2.86-2.65 (m, 9H, $SCH_2CH_2OCH_2CH_2S$ (8H), H-6"), 2.48 (dt, J_1 = 12.6 Hz, J_2 = 4.2 Hz, 1H, H-2eq), 2.34 (m, 2H, H-21, H-16), 2.22 (m, 2H, H-16, H-3eq), 2.00 (s, 3H, $SC\underline{H}_3$), 1.98-1.82 (m, 3H, H-2ax, H-3ax, H-17), 1.38-1.19 (m, 4H, H-18 (2H) H-19 (2H)), 1.14 (d, *J* = 6.9 Hz, 3H, H-14), 0.81 (m, 3H, H-20) (Fig. S17). ^{13}C NMR (125 MHz, D_2O) δ

169.3, 162.8 (q, J = 35.6 Hz, $\underline{C}F_3CO_2H$), 116.3 (q, J = 291.7 Hz, $\underline{C}F_3CO_2H$), 100.7, 94.5, 88.4, 83.8, 77.6, 74.2, 72.6, 72.3, 70.5, 70.3 (2C), 69.7, 69.2, 68.6, 68.4, 68.0 (2C), 67.7, 64.4, 62.9 (2C), 54.6, 50.4, 49.5, 48.3, 47.8, 41.0, 40.4, 39.8, 37.5, 37.2, 35.8, 33.4, 32.7, 31.8, 30.0, 29.3, 27.8, 20.5, 14.5, 13.5, 13.3, 13.2 (Fig. S18). HRMS (ESI) *m/z* calcd for $C_{44}H_{85}N_7O_{15}S_5$ $[M+H]^+$ 1112.4786, found 1112.4791.

Compound 19

Cs_2CO_3 (79 mg, 0.24 mmol), compound **12** (70 mg, 0.24 mmol), and catalytic amount of TBAI were added to compound **5** (265 mg, 0.24 mmol) dissolved in anhydrous THF (1 mL). The reaction mixture was stirred at 40 °C. The reaction progress was monitored by TLC (25:5:75/EtOAc:MeOH:CH_2Cl_2). After 16 h, the reaction mixture was partitioned between H_2O and EtOAc. The organic layer was washed with brine, dried over $MgSO_4$, and concentrated under reduced pressure. Purification by flash chromatography (SiO_2, 90:5:5 to 70:25:5/CH_2Cl_2:EtOAc:MeOH) afforded **19** (235 mg, 73%) as a white solid. ^{1}H NMR (400 MHz, CD_3OD) δ 8.20 (d, J = 8.6 Hz, 1H, H-7), 7.67 (d, J = 8.8 Hz, 1H, H-8), 5.17 (d, J = 2.6 Hz, 1H, H-9), 5.11 (br s, 1H, H-1'), 5.05 (d, J = 3.7 Hz, 1H, H-1"), 4.19 (ddd, J_1 = 7.8 Hz, J_2 = 6.1 Hz, J_3 = 2.6 Hz, 1H, H-10), 4.11 (m, 1H, H-5"), 3.79 (dd, J_1 = 10.8 Hz, J_2 = 7.3 Hz, 1H, H-11), 3.78-3.33 (m, 17H, H-11, H-2', H-4', H-5', H-6', H-1, H-3, H-4, H-5, H-6, H-3", H-2", H-4", $SCH_2CH_2OCH_2CH_2S$ (4H)), 3.26-3.13 (m, 3H, H-12, H-6'), 3.04 (m, 1H, H-6"), 2.83-2.66 (m, 2H, $SCH_2CH_2OCH_2CH_2S$), 2.74-2.66 (m, 1H, H-6"), 2.51 (t, J = 6.3 Hz, 2H, $SCH_2CH_2OCH_2CH_2S$), 2.14 (d, J = 12.9 Hz, 1H, H-2eq), 2.04 (m, 1H, H-3eq), 1.70-1.59 (m, 2H, H-3ax, H-2ax), 1.45 (m, 45H, $5xCO_2C(CH_3)_3$). ^{13}C NMR (100 MHz, CD_3OD) δ 170.8 (2C), 158.0, 157.8, 156.5, 156.3, 150.6, 147.1, 126.9 (2C), 122.8 (2C), 98.3, 98.0, 82.6, 80.9, 79.0 (4C), 75.6, 72.5, 72.1, 70.7, 70.5, 70.2, 69.9, 65.1, 61.1, 58.1, 56.6, 55.6, 50.1, 49.7, 49.5, 40.6, 35.0, 34.4, 33.6, 32.9, 32.0, 31.2, 27.4 (15C). LRMS (ESI) *m/z* calcd for $C_{58}H_{98}N_7O_{24}S_2$ $[M+H]^+$ 1340.60, found 1340.67.

Compound 20

Neat TFA (0.7 mL) was added to compound **19** (30 mg, 0.022 mmol) at rt. After 3 min, the TFA was removed under reduced pressure, and the product was re-dissolved in a minimal volume of H_2O and freeze-dried to afford **20** (32 mg, quant.) as a white foam. Purity = 99% (Table S2 and Fig. S34). ^{1}H NMR (400 MHz, D_2O) δ 8.12 (d, J = 8.7 Hz, 1H, H-7), 7.52 (d, J = 8.5 Hz, 1H, H-8), 5.63 (d, J = 3.6 Hz, 1H, H-1'), 5.07 (d, J = 2.9 Hz, 1H, H-9), 4.97 (d, J = 3.7 Hz, 1H, H-1"), 4.14 (td, J_1 = 6.5 Hz, J_2 = 2.9 Hz, 1H, H-10), 3.92-3.59 (m, 10H, H-2", H-4", H-5", H-11, H-4', H-5', H-4, H-5, H-6), 3.59-3.24 (m, 9H, H-2', H-3", H-6', H-1, H-3, $SCH_2CH_2OCH_2CH_2S$ (4H)), 3.16-3.02 (m, 3H, H-12a, H-12b, H-6'), 2.96 (dd, J_1 = 14.2 Hz, J_2 = 2.5 Hz, 1H, H-6"), 2.66 (m, 3H, $SCH_2CH_2OCH_2CH_2S$ (2H), H-6"), 2.44 (dt, J_1 = 12.6 Hz, J_2 = 4.3 Hz, 1H, H-2eq), 2.34 (dt, J_1 = 13.6 Hz, J_2 = 6.4 Hz, 1H, $SCH_2CH_2OCH_2CH_2S$), 2.25 (dt, J_1 = 13.6 Hz, J_2 = 6.3 Hz, 1H, $SCH_2CH_2OCH_2CH_2S$), 2.18 (dt, J_1 = 12.0 Hz, J_2 = 4.3 Hz, 1H, H-3eq), 1.87 (q, J = 12.0 Hz, 1H, H-3ax), 1.82 (q, J = 12.6 Hz, 1H, H-2ax) (Fig. S19). ^{13}C NMR (100 MHz, D_2O) δ 172.4, 162.7 (q, J = 35.9 Hz, CF_3CO_2H), 149.4, 147.0, 127.0 (2C), 123.6 (2C), 116.2 (q, J = 291.4 Hz, CF_3CO_2H), 100.6, 94.5, 83.9, 77.6, 74.3, 72.6, 70.8, 69.1, 68.8, 68.0, 64.4, 61.3, 58.1 (2C), 56.5, 54.7, 49.5, 48.3, 47.9, 39.8, 34.9, 32.7, 31.8, 31.0, 29.3, 27.8 (Fig. S20). HRMS (ESI) *m/z* calcd for $C_{33}H_{57}N_7O_{14}S_2$ $[M+H]^+$ 840.3483, found 840.3841.

Compound 21

A solution of **13** (40 mg, 0.10 mmol) in MeOH (1.5 mL) was added to a solution of **7** (135 mg, 0.11 mmol) in MeOH (1.5 mL), and the reaction was stirred at 23 °C. The reaction progress was monitored by TLC (95:5/CH_2Cl_2:MeOH). Upon completion, the solvent was removed under reduced pressure. Purification by flash chromatography (SiO_2, 99:1 to 94:6/

CH_2Cl_2:MeOH) afforded **21** (120 mg, 80%) as a white solid. ^{1}H NMR (500 MHz, CD_3OD) δ 8.22 (d, *J* = 8.7 Hz, 1H, H-7), 7.70 (d, *J* = 8.8 Hz, 1H, H-8), 5.19 (d, *J* = 2.6 Hz, 1H, H-9), 5.15 (br s, 1H, H-1'), 5.08 (d, *J* = 3.5 Hz, 1H, H-1"), 4.21 (ddt, J_1 = 7.9 Hz, J_2 = 6.2 Hz, J_3 = 2.7 Hz, 1H, H-10), 4.13 (ddd, J_1 = 9.5 Hz, J_2 = 6.4 Hz, J_3 = 2.7 Hz, 1H, H-5"), 3.84-3.58 (m, 16H, H-11, H-2', H-4', H-5', H-4, H-5, H-6, $SCH_2CH_2OCH_2CH_2S$ (8H)), 3.54-3.43 (m, 5H, H-1, H-3, H-2", H-4", H-6'), 3.23 (d, *J* = 14.8 Hz, 1H, H-12), 3.17 (d, *J* = 15.0 Hz, 1H, H-12), 3.07 (dd, J_1 = 14.4 Hz, J_2 = 2.6 Hz, 1H, H-6"), 3.01-2.89 (m, 4H, $SCH_2CH_2OCH_2CH_2S$), 2.88-2.76 (m, 2H, $SCH_2CH_2OCH_2CH_2S$), 2.73 (m, 1H, H-6"), 2.54 (t, *J* = 6.3 Hz, 2H, $SCH_2CH_2OCH_2CH_2S$), 2.17 (m, 1H, H-2eq), 2.04 (m, 1H, H-3eq), 1.74-1.58 (m, 2H, H-2ax, H-3ax), 1.57-1.37 (m, 45H, $5xCO_2C(CH_3)_3$). ^{13}C NMR (125 MHz, CD_3OD) δ 170.8 (2C), 156.3(2C), 150.6, 147.1, 126.9 (2C), 122.8 (2C), 97.9 (2C), 79.3 (2C), 79.1, 79.0, 78.8, 75.7, 72.6, 72.1, 70.7, 69.8, 68.7 (2C), 68.7, 65.0, 61.1, 56.6, 55.6, 49.5, 40.6, 38.2, 38.1, 38.0, 35.0, 33.7, 32.9, 32.1, 31.2, 27.4 (15C). LRMS (ESI) *m/z* calcd for $C_{62}H_{105}N_7O_{25}S_4Na$ $[M+Na]^+$ 1498.59 found 1498.36.

Compound 22

Neat TFA (0.7 mL) was added to compound **21** (30 mg, 0.02 mmol) at rt. After 3 min, the TFA was removed under reduced pressure, and the product was re-dissolved in a minimal volume of H_2O and freeze-dried to afford **22** (32 mg, quant.) as a white foam. Purity > 99% (Table S2 and Fig. S35). ^{1}H NMR (400 MHz, CD_3OD) δ 8.22 (d, *J* = 8.7 Hz, 1H, H-7), 7.69 (d, *J* = 8.8 Hz, 1H, H-8), 5.79 (d, *J* = 3.1 Hz, 1H, H-1'), 5.18 (d, *J* = 2.6 Hz, 1H, H-9), 5.08 (d, *J* = 3.7 Hz, 1H, H-1"), 4.21 (td, J_1 = 6.1 Hz, J_2 = 3.0 Hz, 1H, H-10), 4.15 (m, 1H, H-4), 3.99 (m, 2H, H-5', H-5"), 3.87 (m, 2H, H-2", H-5), 3.84-3.67 (m, 7H, H-6, H-11, $SCH_2CH_2OCH_2CH_2S$ (4H)), 3.65-3.57 (m, 9H, H-1, H-3, H-4", H-2', H-4', $SCH_2CH_2OCH_2CH_2S$ (4H)), 3.47-3.36 (m, 2H, H-3", H-6'), 3.28-3.06 (m, 4H, H-12, H-6", H-6'), 2.92 (m, 4H, $SCH_2CH_2OCH_2CH_2S$), 2.83-2.79 (m, 2H, $SCH_2CH_2OCH_2CH_2S$), 2.82 (m, 1H, $SCH_2CH_2OCH_2CH_2S$), 2.76 (ddd, J_1 = 14.2 Hz, J_2 = 7.5 Hz, J_3 = 3.4 Hz, 1H, H-6"), 2.60-2.51 (m, 2H, $SCH_2CH_2OCH_2CH_2S$ (1H), H-2eq), 2.23 (dt, J_1 = 11.9 Hz, J_2 = 4.5 Hz, 1H, H-3eq), 1.87 (q, *J* = 11.9 Hz, 1H, H-3ax), 1.84 (q, *J* = 12.6 Hz, 1H, H-2ax) (Fig. S21). ^{13}C NMR (100 MHz, D_2O) δ 173.1, 163.6 (q, *J* = 35.9 Hz, CF_3CO_2H), 150.0, 147.7, 127.7 (2C), 124.3 (2C), 117.0 (q, *J* = 291.6 Hz, CF_3CO_2H), 101.4, 95.2, 84.6, 78.2, 74.9, 73.3, 73.2, 73.0, 71.4, 71.0, 69.9, 69.6, 68.6 (2C), 65.1, 61.9, 57.2, 55.3, 50.2, 49.0, 48.6, 40.8, 40.5, 38.6, 35.7, 33.4, 32.6, 31.7, 30.0, 28.5 (Fig. S22). HRMS (ESI) *m/z* calcd for $C_{37}H_{65}N_7O_{15}S_4$ $[M+H]^+$ 976.3500, found 976.3506.

Compound 23

Cs_2CO_3 (27 mg, 0.08 mmol), compound **12** (49 mg, 0.170 mmol), and a catalytic amount of TBAI were added to compound **9** (45 mg, 0.085 mmol) dissolved in anhydrous THF (1 mL). The reaction mixture was stirred at 40 °C. The reaction progress was monitored by TLC (2:1:7/EtOAc:MeOH:CH_2Cl_2). After 16 h, the reaction mixture was partitioned between H_2O and EtOAc. The organic layer was washed with brine, dried over $MgSO_4$, and concentrated under reduced pressure. Purification by flash chromatography (SiO_2, 9:1/ CH_2Cl_2:EtOAc to 8:1:1/CH_2Cl_2:EtOAc:MeOH) afforded **23** (47 mg, 71%) as a white solid. Purity = 98% (Table S2 and Fig. S36). ^{1}H NMR (400 MHz, CD_3OD) δ 8.21 (d, *J* = 8.8 Hz, 2H, H-9), 7.7 (d, *J* = 8.9 Hz, 2H, H-10), 5.28 (d, *J* = 5.7 Hz, 1H, H-1), 5.18 (d, *J* = 2.7 Hz, 1H, H-11), 4.44 (dd, J_1 = 9.5 Hz, J_2 = 3.9 Hz, 1H, H-6), 4.27-4.16 (m, 2H, H-5, H-12), 4.12 (dd, J_1 = 10.2 Hz, J_2 = 5.6 Hz, 1H, H-2), 3.82-3.74 (m, 2H, H-4, H-13), 3.66-3.54 (m, 6H, H-3, H-13, $SCH_2CH_2OCH_2CH_2S$ (4H)), 3.40 (dd, J_1 = 7.1 Hz, J_2 = 3.9 Hz, 1H, H-7), 3.26-3.11 (m, 3H, H-9, H-14 (2H)), 2.99 (dd, J_1 = 10.5 Hz, J_2 = 5.0 Hz, 1H, H-5'), 2.85 (dt, J_1 = 13.6 Hz, J_2 = 6.5 Hz, 1H, $SCH_2CH_2OCH_2CH_2S$), 2.74 (dt, J_1 = 13.6 Hz, J_2 = 6.5 Hz, 1H, $SCH_2CH_2OCH_2CH_2S$), 2.55 (t, *J* = 6.3 Hz, 2H, $SCH_2CH_2OCH_2CH_2S$), 2.45 (s, 3H, $NC\underline{H}_3$), 2.21-2.15 (m, 1H, H-5'), 2.14 (s, 3H, $SC\underline{H}_3$), 2.10-1.96 (m, 2H, H-3' (2H)), 1.86 (m,

1H, H-4'), 1.47-1.28 (m, 4H, H-1" (2H), H-2" (2H)), 1.29 (d, J = 7.1 Hz, 1H, H-8), 0.94 (m, 3H, H-3") (Fig. S23). ^{13}C NMR (100 MHz, CD_3OD) δ 178.4, 172.3, 152.1, 148.5, 128.4 (2C), 124.2 (2C), 90.3, 72.1, 71.7, 71.3, 70.8, 70.5, 70.2, 70.1, 70.0, 69.5, 63.8, 62.5, 58.1, 52.0, 42.1, 41.2, 39.7, 39.5, 38.9, 38.7, 37.1, 36.5, 32.7, 31.3, 22.6, 15.5, 14.6, 14.1 (Fig. S24). HRMS (ESI) *m/z* calcd for $C_{33}H_{54}N_4O_{11}S_3$ $[M+H]^+$ 779.3029, found 779.3031.

Compound 24

A solution of **14** (95 mg, 0.18 mmol) in MeOH (2.5 mL) was added to a solution of **9** (90 mg, 0.18 mmol) in MeOH (2.5 mL), and the reaction was stirred at 23 °C. The reaction progress was monitored by TLC (9:1/CH_2Cl_2:MeOH). Upon completion, the solvent was removed under reduced pressure. Purification by flash chromatography (SiO_2, 99:1 to 88:12/CH_2Cl_2:MeOH) afforded **24** (132 mg, 80%) as a white solid. Purity > 99% (Table S2 and Fig. S37). ^{1}H NMR (400 MHz, CD_3OD) δ 8.21 (d, J = 8.8 Hz, 2H, H-9), 7.69 (d, J = 8.4 Hz, 2H, H-10), 5.28 (d, J = 5.6 Hz, 1H, H-1), 5.18 (d, J = 2.6 Hz, 1H, H-11), 4.44 (dd, J_1 = 9.6 Hz, J_2 = 3.8 Hz, 1H, H-6), 4.23-4.17 (m, 2H, H-5, H-12), 4.12 (dd, J_1 = 10.2 Hz, J_2 = 5.6 Hz, 1H, H-2), 3.83-3.52 (m, 11H, H-4, H-13 (2H), $SCH_2CH_2OCH_2CH_2S$ (8H)), 3.43 (dp, J_1 = 7.1 Hz, J_2 = 3.6 Hz, 1H, H-7), 3.26-3.10 (m, 3H, H-9, H-14 (2H)), 3.00 (dd, J_1 = 10.6 Hz, J_2 = 4.9 Hz, 1H, H-5'a), 2.93 (m, 4H, $SCH_2CH_2OCH_2CH_2S$), 2.84 (dt, J_1 = 13.8 Hz, J_2 = 6.4 Hz, 1H, $SCH_2CH_2OCH_2CH_2S$), 2.72 (dt, J_1 = 13.8 Hz, J_2 = 6.4 Hz, 1H, $SCH_2CH_2OCH_2CH_2S$), 2.55 (td, J_1 = 6.3 Hz, J_2 = 1.9 Hz, 2H, $SCH_2CH_2OCH_2CH_2S$), 2.45 (s, 3H, $NC\underline{H}_3$), 2.22-2.16 (m, 1H, H-5'b), 2.15 (s, 3H, $SC\underline{H}_3$), 2.11-1.96 (m, 2H, H-3' (2H)), 1.86 (m, 1H, H-4'), 1.45-1.31 (m, 4H, H- 1" (2H), H-2" (2H)),1.27 (d, J = 7.1 Hz, H-8), 0.98-0.92 (m, 3H, H-3") (Fig. S25). ^{13}C NMR (100 MHz, CD_3OD) δ 178.4, 172.2, 152.0, 148.5, 128.3 (2C), 124.2 (2C), 90.3, 72.0, 71.6, 71.3, 70.8, 70.4, 70.1, 70.0, 69.9, 69.5, 63.8, 62.5, 58.0, 51.9, 42.0, 41.2, 39.6, 39.5, 38.9, 38.7, 37.0, 36.4, 32.6, 31.2, 22.6, 15.4, 14.5, 14.0 (Fig. S26). HRMS (ESI) *m/z* calcd for $C_{37}H_{62}N_4O_{12}S_5$ $[M+H]^+$ 915.3046, found 915.3052.

Compound 25

Cs_2CO_3 (33 mg, 0.1 mmol), compound **12** (30 mg, 0.1 mmol), and a catalytic amount of TBAI were added to compound **13** (40 mg, 0.1 mmol) dissolved in anhydrous THF (1 mL). The reaction mixture was stirred at 40 °C. The reaction progress was monitored by TLC (96:4/EtOAc:MeOH). After 16 h, the reaction mixture was partitioned between H_2O and EtOAc. The organic layer was washed with brine, dried over $MgSO_4$, and concentrated under reduced pressure. Purification by flash chromatography (SiO_2, 6:4/petroleum ether: EtOAc to 96:4/EtOAc:MeOH) afforded **25** (45 mg, 68%) as a white solid. Purity = 98% (Table S2 and Fig. S38). ^{1}H NMR (400 MHz, CD_3OD) δ 8.21 (d, J = 8.7 Hz, 4H, H-1), 7.69 (d, J = 8.5 Hz, 4H, H-2), 5.17 (d, J = 2.7 Hz, 2H, H-3), 4.20 (m, 1H, H-4), 3.80 (dd, J_1 = 10.8 Hz, J_2 = 7.3 Hz, 2H, H-5), 3.62 (dd, J_1 = 10.6 Hz, J_2 = 5.9 Hz, 2H, H-5), 3.54 (t, J = 6.2 Hz, 4H, $SCH_2CH_2OCH_2CH_2S$), 3.22 (d, J = 14.9 Hz, 2H, H-6), 3.16 (d, J = 14.9 Hz, 2H, H-6), 2.54 (t, J = 6.2 Hz, 4H, $SCH_2CH_2OCH_2CH_2S$) (Fig. S27). ^{13}C NMR (100 MHz CD_3OD) δ 172.3 (2C), 152.0 (2C), 148.6 (2C), 128.4 (4C), 124.2 (4C), 71.4 (4C), 62.5 (2C), 58.1 (2C), 36.4 (2C), 32.7 (2C) (Fig. S28). HRMS (ESI) *m/z* calcd for $C_{26}H_{34}N_4O_{11}S_2$ $[M+Na]^+$ 665.1563, found 665.1576.

Compound 26

A solution of **14** (40 mg, 0.060 mmol) in MeOH (2 mL) was added to a solution of **13** (35 mg, 0.089) in MeOH (2 mL), and the reaction was stirred at 23 °C. The reaction progress was monitored by TLC (96:4/EtOAc:MeOH). Upon completion, the solvent was removed under reduced pressure. Purification by flash chromatography (SiO_2, 6:4/petroleum ether: EtOAc to 96:4/EtOAc:MeOH) afforded **26** (56 mg, 89%) as a white solid. Purity = 97%

(Table S2 and Fig. S39). ^{1}H NMR (500 MHz, CD_3OD) δ 8.22 (d, J = 8.8 Hz, 4H, H-1), 7.68 (d, J = 8.5 Hz, 4H, H-2), 5.18 (d, J = 2.7 Hz, 2H, H-3), 4.20 (ddd, J_1 = 7.6 Hz, J_2 = 5.8 Hz, J_3 = 2.7 Hz, 2H, H-4), 3.80 (dd, J_1 = 10.8 Hz, J_2 = 7.4 Hz, 2H, H-5'), 3.70 (t, J = 6.4 Hz, 4H, $SCH_2CH_2OCH_2CH_2S$), 3.65 (dd, J_1 = 10.7 Hz, J_2 = 5.9 Hz, 2H, H-5'), 3.59 (m, 4H, $SCH_2CH_2OCH_2CH_2S$), 3.23 (d, J = 14.9 Hz, 2H, H-6), 3.16 (d, J = 14.9, 2H, H-6), 2.92 (t, J = 6.3 Hz, 4H, $SCH_2CH_2OCH_2CH_2S$), 2.54 (t, J = 6.3 Hz, 4H, $SCH_2CH_2OCH_2CH_2S$) (Fig. S29). ^{13}C NMR (125 MHz, CD_3OD) δ 172.3 (2C), 152.1 (2C), 148.5 (2C), 128.3 (4C), 124.2 (4C), 71.7 (2C), 71.3 (2C), 70.1 (2C), 62.5 (2C), 58.1 (2C), 39.5 (2C), 36.4 (2C), 32.7 (2C) (Fig. S30). HRMS (ESI) *m/z* calcd for $C_{30}H_{42}N_4O_{12}S_4$ $[M+Na]^+$ 801.1580, found 801.1588.

Preparation of the pCNR-Int-pET19b-pps overexpression construct

H. influenzae ATCC 51907 genomic DNA was isolated using the Wizard Genomic DNA purification kit by following the Promega protocol for Gram-negative bacterial samples. To construct the pCNR-Int-pET19b-pps plasmid encoding the chloramphenicol nitroreductase (CNR), PCR was performed using *H. influenzae* ATCC 51907 genomic DNA as a template, the forward primer (GGAAATCATATGACTCAACTTACTCGT), the reverse primer (TTAATGCTCGAGTTACCCCACCCATTT), and Phusion DNA polymerase. The resulting DNA fragment was inserted into the linearized Int-pET19b-pps by using the corresponding *Nde*I and *Xho*I restriction sites (underlined in the primers). The resulting plasmid was transformed into *E. coli* TOP10 chemically competent cells. The plasmid bearing the CNR gene insert was sequenced and showed perfect alignment with the reported sequence (locus tag HI1278).

Preparation of the pCPT-Int-pET19b-pps overexpression construct

To construct the pCPT-Int-pET19b-pps plasmid encoding the chloramphenicol phosphotransferase (CPT), PCR was performed using pCPT-pET16b as a template, the forward primer (CCCTCTCATATGATCATCCTCAACGGC), the reverse primer (GCAGCCCTCGAGCTACGGGACGACGTG), and Phusion DNA polymerase. The resulting DNA fragment was inserted into the linearized Int-pET19b-pps by using the corresponding *Nde*I and *Xho*I restriction sites (underlined in the primers). The resulting plasmid was transformed into *E. coli* TOP10 chemically competent cells. The plasmid bearing the CPT gene insert was sequenced and showed perfect alignment with the reported sequence (locus tag SVEN_4064).

Overproduction and purification of chloramphenicol-modifying enzymes

The CNR and CPT enzymes (with $NHis_{10}$ tags) were prepared in a similar manner. To produce a large amount of protein, the pCNR-Int-pET19b-pps and pCPT-Int-pET19b-pps vectors were transformed into *E. coli* BL21 (DE3) chemically competent cells. For protein overexpression, a 10-mL portion of an overnight culture was used as an inoculum for 1-L of culture of LB supplemented with ampicillin (100 μg/mL). Cells were grown to an absorbance of 0.6 at 600 nm, at which point protein expression was induced with 1 mM IPTG (final concentration). Cultures were incubated overnight at 20 °C. Cells were collected, lysed, and protein was purified by Ni^{II}-NTA affinity chromatography as we previously reported for the purification of ANT(4').[41] After purification, the proteins were dialyzed in 50 mM Tris-HCl (pH 8.0), 100 mM NaCl, and 10% v/v glycerol and flash frozen in liquid N_2 for storage at −80 °C. CNR was obtained in yields of 3.8 mg/L of culture, and CPT was obtained at 1.4 mg/L of culture (Fig. S40).

Determination of the CNR cofactor

In order to determine the CNR cofactor (FMN or FAD), a sample of the CNR enzyme was boiled (10 min), and the precipitated protein was removed by centrifugation (13,000 rpm, 10 min, rt). The supernatant was split into aliquots (100 μL) into a 96-well plate. Snake venom from *Naja naja kaouthia* (Sigma V9125) resuspended in 50 mM Tris, pH 8.0 (adding just enough buffer so that the venom was not yellow, ~5 μL) was then added to the supernatant and the fluorescence (ex. 450 nm; em. 520 nm) of FMN was monitored every minute for 30 min. FMN (100 μL, 0.1 mM and 0.5 mM) and FAD (100 μL, 0.1 mM and 0.5 mM), treated with snake venom exactly as was the CNR supernatant, were utilized as controls. An increase in fluorescence was observed for the FAD controls, whereas no change in fluorescence was observed for the FMN controls or the boiled CNR enzyme supernatant, leading to the conclusion that FMN is the cofactor bound to the CNR.

Determination of MIC values of antibiotic compounds

MIC values were determined against a variety of Gram-positive and Gram-negative bacterial strains: *B. subtilis* 168 (A), *B. subtilis* 168 with AAC(6')/APH(2")-pRB374 (B), *M. smegmatis* str. MC2 155 (C), *B. cereus* ATCC 11778 (D), *L. monocytogenes* ATCC 19115 (E), *S. aureus* ATCC 29213 (F), *S. aureus* NorA (G), *E. coli* MC1061 (H), *B. anthracis* 34F2 Sterne strain (I), *H. influenzae* ATCC 51907 (J), *S. epidermidis* ATCC 12228 (biofilm negative) (K), and *S. pyogenes* M12 *str*. MGAS9429 (L). Strains were tested using a double-dilution of our compounds. All experiments were performed in duplicate or triplicate.

Determination of activity of compounds as inhibitors of bacterial protein synthesis

Protein translation inhibition was quantified in a coupled transcription/translation assay by using *E. coli* S30 extracts for circular DNA with the pBEST*luc* plasmid (Promega) according to the manufacturer's protocol. Translation reactions (10 μL) containing various concentrations of the tested compounds were incubated at 37 °C for 90 min, cooled on ice for 5 min, and diluted with a dilution reagent (25 mM Tris-phosphate buffer, pH 7.8, 2 mM DTT, 2 mM 1,2-diaminocyclohexanetetraacetate, 10% glycerol, 1% Triton X-100, and 1 mg/mL BSA) into 96-well plates. The luminescence was measured immediately after the addition of the luciferase assay reagent (25 μL; Promega), and the light emission was recorded by using a Victor3 plate reader (Perkin-Elmer). The concentrations of half-maximal inhibition (IC_{50}) values were obtained from concentration-response curves fitted to the data of at least two independent experiments by using Grafit 5 software.

Determination of antibiotic-modifying enzyme activity on our antibiotics compounds

Several previously developed assays were employed to visualize the transformation of the compounds by antibiotic-modifying enzymes. All reactions were monitored at 25 °C on a SpectraMax M5 microplate reader and performed in triplicate. All rates were normalized to the parent compound.

Acetylation—The activity of several acetyltransferase enzymes (AAC(6')/APH(2"),[42] AAC(6')-Ib',[43] AAC(3)-IV,[42] AAC(2')-Ic,[44] Eis,[44] and CAT_I[45]) was monitored at 412 nm using Ellman's method, coupling the release of CoASH with DTNB. Due to the reactivity of the thiol moiety in the acetylation assay, compounds **6, 9**, and **13** bearing free thiols were not tested in this assay. Briefly, reactions (200 μL) containing antibiotic compounds (100 μM), AcCoA (500 μM for Eis and 150 μM for other acetyltransferases) were incubated with acetyltransferase enzyme (0.125 μM AAC(3)-IV and AAC(2')-Ic, 0.5 μM for other acetyltransferases) in the presence of DTNB (2 mM) and the appropriate buffer (50 mM MES pH 6.6 for AAC(6')/APH(2") and AAC(3)-IV; 50 mM Tris pH 7.5 for AAC(6')-Ib'; 100 mM sodium phosphate pH 7.4 for AAC(2')-Ic; and 50 mM Tris pH 8.0 for Eis and

CAT_I). Measurements were taken every 30 sec for 1 h. Initial rates of the reactions were calculated using data from the first 2–5 min of the reaction.

Nucleotidylation—The nucleotidylation activity of ANT(4') from *S. aureus* was monitored through the formation of a complex of molybdate, malachite green, and the inorganic phosphate (P_i) generated by inorganic pyrophosphatase (Sigma-Aldrich catalog #I1643) cleavage of the released pyrophosphate (PP_i) during the nucleotidylation reaction.[41] To analyze the activity of ANT(4') on compounds **1, 6, 16, 18, 20**, and **22**, reactions (160 μL) containing Tris-HCl (50 mM, pH 7.5), $MgCl_2$ (10 mM), KCl (40 mM), inorganic pyrophosphatase (0.2 U/mL), antibiotic compound (100 μM), and ATP (0.5 mM) were performed at 25 °C. The reactions were initiated by the addition of the enzyme (1 μM), incubated for 20, 40, 60, 120, and 140 s, and quenched by the addition of the malachite green reagent (40 μL). After 15 min of color development, the liberated P_i concentration was measured at 600 nm. The initial rates were determined using the first 60 sec of the reaction.

Phosphorylation—The phosphorylation activity of CPT was monitored at 340 nm through the consumption of NADH in an enzyme-coupled response to the production of ADP.[46] Reactions (250 μL total volume) contained 100 μM antibiotic compound, 50 mM Tris-HCl (pH 8.0), 10 mM $MgCl_2$, 40 mM KCl, 0.5 mg/mL NADH, 2.5 mM PEP, 2 mM ATP, and 5 μL PK/LDH, and were initiated by addition of 1 μM CPT. The progress of the reaction was monitored by taking readings every 30 sec for 1 h. The initial rates were determined using the first 5 min of the reaction.

Reduction—The reduction activity of CNR was monitored at 340 nm through the consumption of NADH used to reduce the FMN in the active site of CNR. Reactions (200 μL total volume) contained 100 μM antibiotic compound, 50 mM Tris-HCl (pH 7.5) and 0.5 mg/mL NADH and were initiated by addition of 0.5 μM CNR. Reaction progress was monitored every 30 sec for 1 h. The initial rates were determined using the first 5 min of the reaction.

Supplementary Material

Refer to Web version on PubMed Central for supplementary material.

Acknowledgments

This work was supported by a National Institutes of Health Grant AI090048 (to S.G.-T.) and by a Marie Curie International Reintegration Grant 246673 (to M.F.). We thank Prof. Philip C. Hanna (University of Michigan), Paul Hergenrother (University of Illinois at Urbana-Champaign), David Sherman (University of Michigan), and Sabine Ehrt (Weill Cornell Medical College) for gifts of bacterial strains. We thank Dr. Tapan Biswas (University of Michigan) and Dr. Jacqueline Ellis (University of Leicester) for providing us with vectors and plasmids used for cloning experiments. We thank Prof. Timor Baasov and Mrs. Dana Atia-Glikin for for their generous assistance in conducting the *in vitro* translation assays.

Funding Sources

S.G.-T. was funded by NIH grant AI090048, and M.F. was funded by Marie Curie International Reintegration Grant 246673.

ABBREVIATIONS

AAC	aminoglycoside acetyltransferase
AG	aminoglycoside

AME	aminoglycoside-modifying enzyme
ANT	aminoglycoside nucleotidyltransferase
APH	aminoglycoside phosphotransferase
CAT	chloramphenicol acetyltransferase
CNR	chloramphenicol nitroreductase
CPT	chloramphenicol phosphotransferase

REFERENCES

1. Wright GD. Q&A: Antibiotic resistance: where does it come from and what can we do about it? BMC biology. 2010; 8:123. [PubMed: 20887638]
2. Yonath A. Antibiotics targeting ribosomes: resistance, selectivity, synergism and cellular regulation. Ann Rev Biochem. 2005; 74:649–679. [PubMed: 16180279]
3. Sutcliffe JA. Antibiotics in development targeting protein synthesis. Ann NY Acad Sci. 2011; 1241:122–152. [PubMed: 22191530]
4. Tenson T, Mankin A. Antibiotics and the ribosome. Molec Microbiol. 2006; 59:1664–1677. [PubMed: 16553874]
5. Carter AP, Clemons WM, Brodersen DE, Morgan-Warren RJ, Wimberly BT, Ramakrishnan V. Functional insights from the structure of the 30S ribosomal subunit and its interactions with antibiotics. Nature. 2000; 407:340–348. [PubMed: 11014183]
6. Brodersen DE, Clemons WM Jr, Carter AP, Morgan-Warren RJ, Wimberly BT, Ramakrishnan V. The structural basis for the action of the antibiotics tetracycline, pactamycin, and hygromycin B on the 30S ribosomal subunit. Cell. 2000; 103:1143–1154. [PubMed: 11163189]
7. Pioletti M, Schluenzen F, Harms J, Zarivach R, Gluehmann M, Avila H, Bashan A, Bartels H, Auerbach T, Jacobi C, Hartsch T, Yonath A, Franceschi F. Crystal structures of complexes of the small ribosomal subunit with tetracycline, edeine and IF3. EMBO J. 2001; 20:1829–1839. [PubMed: 11296217]
8. Dunkle JA, Xiong L, Mankin AS, Cate JH. Structures of the Escherichia coli ribosome with antibiotics bound near the peptidyl transferase center explain spectra of drug action. Proc Nat Acad Sci, U.S.A. 2010; 107:17152–17157.
9. Hansen JL, Moore PB, Steitz TA. Structures of five antibiotics bound at the peptidyl transferase center of the large ribosomal subunit. J Molec Biol. 2003; 330:1061–1075. [PubMed: 12860128]
10. Schlunzen F, Zarivach R, Harms J, Bashan A, Tocilj A, Albrecht R, Yonath A, Franceschi F. Structural basis for the interaction of antibiotics with the peptidyl transferase centre in eubacteria. Nature. 2001; 413:814–821. [PubMed: 11677599]
11. Wright GD. Bacterial resistance to antibiotics: enzymatic degradation and modification. Adv Drug Deliv Rev. 2005; 57:1451–1470. [PubMed: 15950313]
12. Webber MA, Piddock LJ. The importance of efflux pumps in bacterial antibiotic resistance. J Antimicrob Chemother. 2003; 51:9–11. [PubMed: 12493781]
13. Li XZ, Nikaido H. Efflux-mediated drug resistance in bacteria. Drugs. 2004; 64:159–204. [PubMed: 14717618]
14. Delcour AH. Outer membrane permeability and antibiotic resistance. Biochim Biophys Acta. 2009; 1794:808–816. [PubMed: 19100346]
15. Long, KS.; Vester, B. EcoSal-Escherichia coli and salmonella: Cellular and molecular biology. Washington, DC: ASM Press; 2008. Chapter 2.5.7: Antibiotic resistance mechanisms, with an emphasis on those related to the ribosome.
16. Auerbach T, Bashan A, Yonath A. Ribosomal antibiotics: structural basis for resistance, synergism and selectivity. Trends Biotechnol. 2004; 22:570–576. [PubMed: 15491801]

17. Douthwaite, S.; Fourmy, D.; Yoshizawa, S. Topics in current genetics, fine-tuning of RNA functions by modification and editing. Berlin, Heidelberg: Springer-Verlag; 2005. Nucleotide methylations in rRNA that confer resistance to ribosome-targeting antibiotics.
18. Chow CS, Lamichhane TN, Mahto SK. Expanding the nucleotide repertoire of the ribosome with post-transcriptional modifications. ACS Chem Biol. 2007; 2:610–619. [PubMed: 17894445]
19. Lee J, Kwon M, Lee KH, Jeong S, Hyun S, Shin KJ, Yu J. An approach to enhance specificity against RNA targets using heteroconjugates of aminoglycosides and chloramphenicol (or linezolid). J Am Chem Soc. 2004; 126:1956–1957. [PubMed: 14971927]
20. Hubschwerlen C, Specklin JL, Baeschlin DK, Borer Y, Haefeli S, Sigwalt C, Schroeder S, Locher HH. Structure-activity relationship in the oxazolidinone-quinolone hybrid series: influence of the central spacer on the antibacterial activity and the mode of action. Bioorg Med Chem Lett. 2003; 13:4229–4233. [PubMed: 14623007]
21. Pokrovskaya V, Baasov T. Dual-acting hybrid antibiotics: a promising strategy to combat bacterial resistance. Expert Opin Drug Discov. 2010; 5:883–902. [PubMed: 22823262]
22. Wimberly BT. The use of ribosomal crystal structures in antibiotic drug design. Curr Opin Investig Drugs. 2009; 10:750–765.
23. Zhou J, Bhattacharjee A, Chen S, Chen Y, Duffy E, Farmer J, Goldberg J, Hanselmann R, Ippolito JA, Lou R, Orbin A, Oyelere A, Salvino J, Springer D, Tran J, Wang D, Wu Y, Johnson G. Design at the atomic level: generation of novel hybrid biaryloxazolidinones as promising new antibiotics. Bioorg Med Chem Lett. 2008; 18:6179–6183. [PubMed: 18951792]
24. Sucheck SJ, Wong AL, Koeller KM, Boehr DD, Draker K-A, Sears P, Wright GD, Wong C-H. Design of bifunctional antibiotics that target bacterial rRNA and inhibit resistance-causing enzymes. J Am Chem Soc. 2000; 122:5230–5231.
25. Kumar S, Arya DP. Recognition of HIV TAR RNA by triazole linked neomycin dimers. Bioorg Med Chem Lett. 2011; 21:4788–4792. [PubMed: 21757341]
26. Kumar S, Kellish P, Robinson WE Jr, Wang D, Appella DH, Arya DP. Click dimers to target HIV TAR RNA conformation. Biochemistry. 2012; 51:2331–2347. [PubMed: 22339203]
27. Michael K, Wang H, Tor Y. Enhanced RNA binding of dimerized aminoglycosides. Bioorg Med Chem. 1999; 7:1361–1371. [PubMed: 10465410]
28. Lee ML, Childs-Disney JL, Pushechnikov A, French JM, Sobczak K, Thornton CA, Disney MD. Controlling the specificity of modularly assembled small molecules for RNA via ligand module spacing: Targeting the RNAs that cause myotonic muscular dystrophy. J Am Chem Soc. 2009; 131:17464–17472. [PubMed: 19904940]
29. Gonzalez LS 3rd, Spencer JP. Aminoglycosides: a practical review. Am Fam Physician. 1998; 58:1811–1820. [PubMed: 9835856]
30. Houghton JL, Green KD, Chen W, Garneau-Tsodikova S. The future of aminoglycosides: the end or renaissance? Chembiochem. 2010; 11:880–902. [PubMed: 20397253]
31. Vicens Q, Westhof E. Crystal structure of a complex between the aminoglycoside tobramycin and an oligonucleotide containing the ribosomal decoding a site. Chem Biol. 2002; 9:747–755. [PubMed: 12079787]
32. Russell NE, Pachorek RE. Clindamycin in the treatment of streptococcal and staphylococcal toxic shock syndromes. Ann Pharmacother. 2000; 34:936–939. [PubMed: 10928407]
33. Bozdogan B, Berrezouga L, Kuo MS, Yurek DA, Farley KA, Stockman BJ, Leclercq R. A new resistance gene, linB, conferring resistance to lincosamides by nucleotidylation in Enterococcus faecium HM1025. Antimicrob Agents Chemother. 1999; 43:925–929. [PubMed: 10103201]
34. Long KS, Poehlsgaard J, Kehrenberg C, Schwarz S, Vester B. The Cfr rRNA methyltransferase confers resistance to Phenicols, Lincosamides, Oxazolidinones, Pleuromutilins, and Streptogramin A antibiotics. Antimicrob Agents Chemother. 2006; 50:2500–2505. [PubMed: 16801432]
35. Neu HC, Fu KP. In vitro activity of chloramphenicol and thiamphenicol analogs. Antimicrob Agents Chemother. 1980; 18:311–316. [PubMed: 7447408]
36. Schwarz S, Kehrenberg C, Doublet B, Cloeckaert A. Molecular basis of bacterial resistance to chloramphenicol and florfenicol. FEMS Microbiol Rev. 2004; 28:519–542. [PubMed: 15539072]
37. Yunis AA. Chloramphenicol toxicity: 25 years of research. American J Med. 1989; 87:44N–48N.

38. Rana VS, Kumar VA, Ganesh KN. Oligonucleotides with (N-thymin-1-ylacetyl)-1-arylserinol backbone: chiral acyclic analogs with restricted conformational flexibility. Tetrahedron. 2001; 57:1311–1321.

39. Herzog IM, Green KD, Berkov-Zrihen Y, Feldman M, Vidavski RR, Eldar-Boock A, Satchi-Fainaro R, Eldar A, Garneau-Tsodikova S, Fridman M. 6'-Thioether tobramycin analogues: towards selective targeting of bacterial membranes. Angew Chem Int Ed Engl. 2012; 51:5652–5656. [PubMed: 22499286]

40. Ellis J, Campopiano DJ, Izard T. Cubic crystals of chloramphenicol phosphotransferase from Streptomyces venezuelae in complex with chloramphenicol. Acta crystallographica. Section D, Biol Crystallog. 1999; 55:1086–1088.

41. Porter VR, Green KD, Zolova OE, Houghton JL, Garneau-Tsodikova S. Dissecting the cosubstrate structure requirements of the Staphylococcus aureus aminoglycoside resistance enzyme ANT(4'). Biochem Biophys Res Commun. 2010; 403:85–90. [PubMed: 21040710]

42. Green KD, Chen W, Houghton JL, Fridman M, Garneau-Tsodikova S. Exploring the substrate promiscuity of drug-modifying enzymes for the chemoenzymatic generation of N-acylated aminoglycosides. Chembiochem. 2010; 11:119–126. [PubMed: 19899089]

43. Green KD, Chen W, Garneau-Tsodikova S. Effects of altering aminoglycoside structures on bacterial resistance enzyme activities. Antimicrob Agents Chemother. 2011; 55:3207–3213. [PubMed: 21537023]

44. Chen W, Biswas T, Porter VR, Tsodikov OV, Garneau-Tsodikova S. Unusual regioversatility of acetyltransferase Eis, a cause of drug resistance in XDR-TB. Proc Nat Acad Sci, U.S.A. 2011; 108:9804–9808.

45. Biswas T, Houghton JL, Garneau-Tsodikova S, Tsodikov OV. The structural basis for substrate versatility of chloramphenicol acetyltransferase CATI. Protein Sci. 2012; 21:520–530. [PubMed: 22294317]

46. Shaul P, Green KD, Rutenberg R, Kramer M, Berkov-Zrihen Y, Breiner-Goldstein E, Garneau-Tsodikova S, Fridman M. Assessment of 6'- and 6'''-N-acylation of aminoglycosides as a strategy to overcome bacterial resistance. Org Biomolec Chem. 2011; 9:4057–4063.

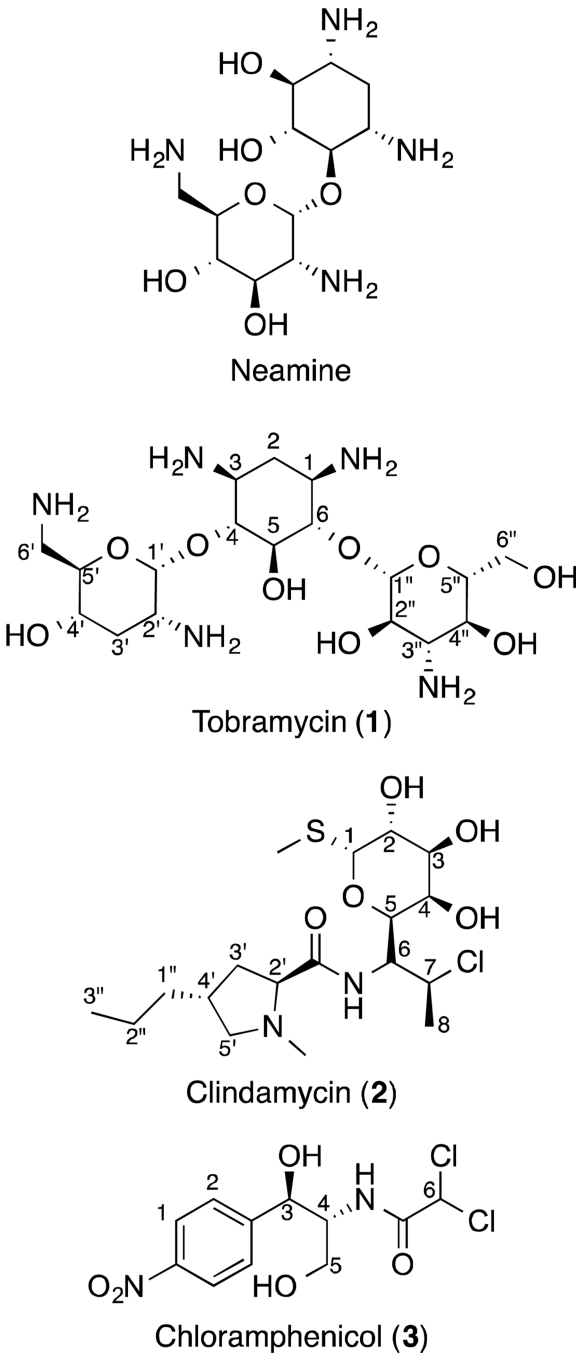

Figure 1.
Structures of neamine, tobramycin (**1**), clindamycin (**2**), and chloramphenicol (**3**).

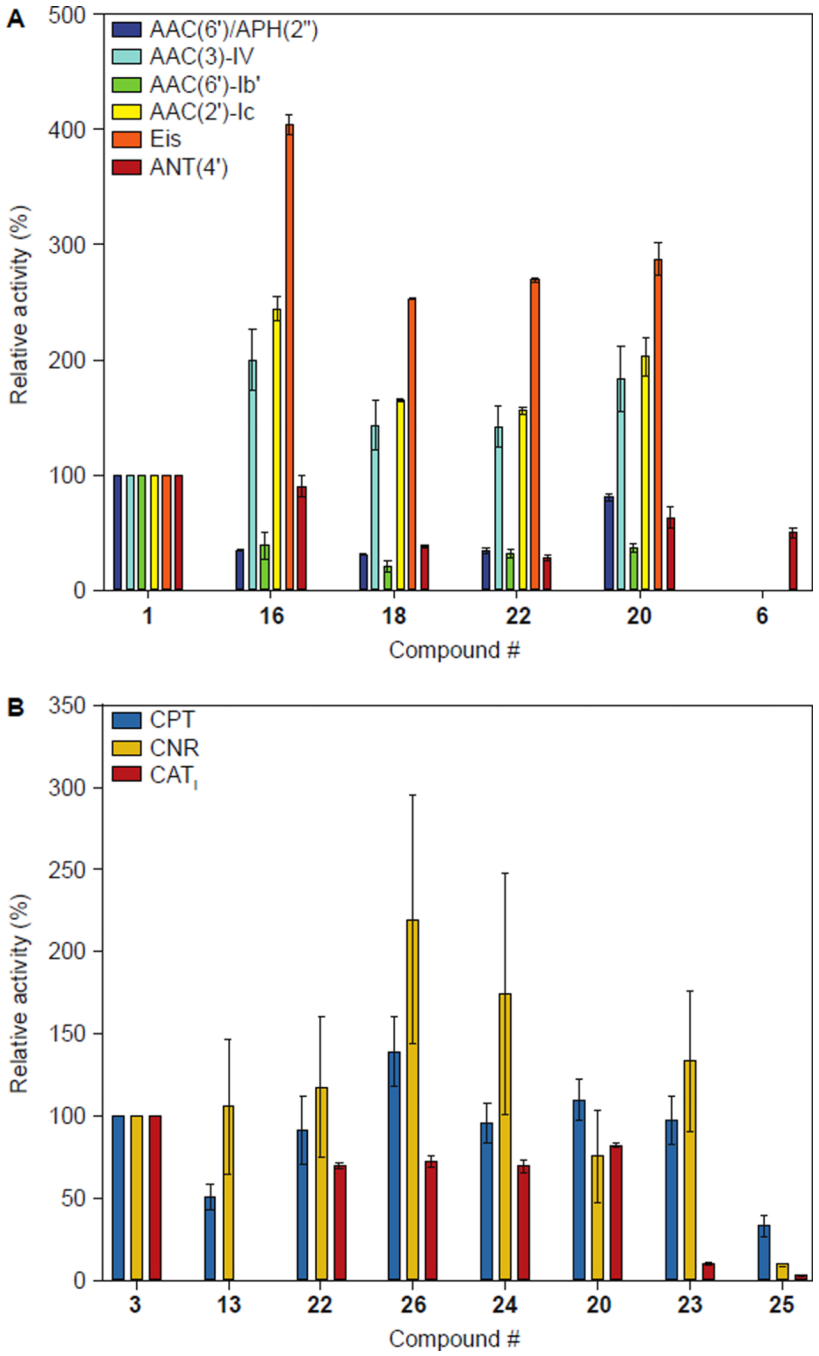

Figure 2.

A. Activities of various AMEs on tobramycin-containing molecules (**6, 16, 18, 20**, and **22**) relative to **1. B**. Activities of various chloramphenicol-modifying enzymes on chloramphenicol -containing molecules (**13, 20, 22–26**) relative to **3**.

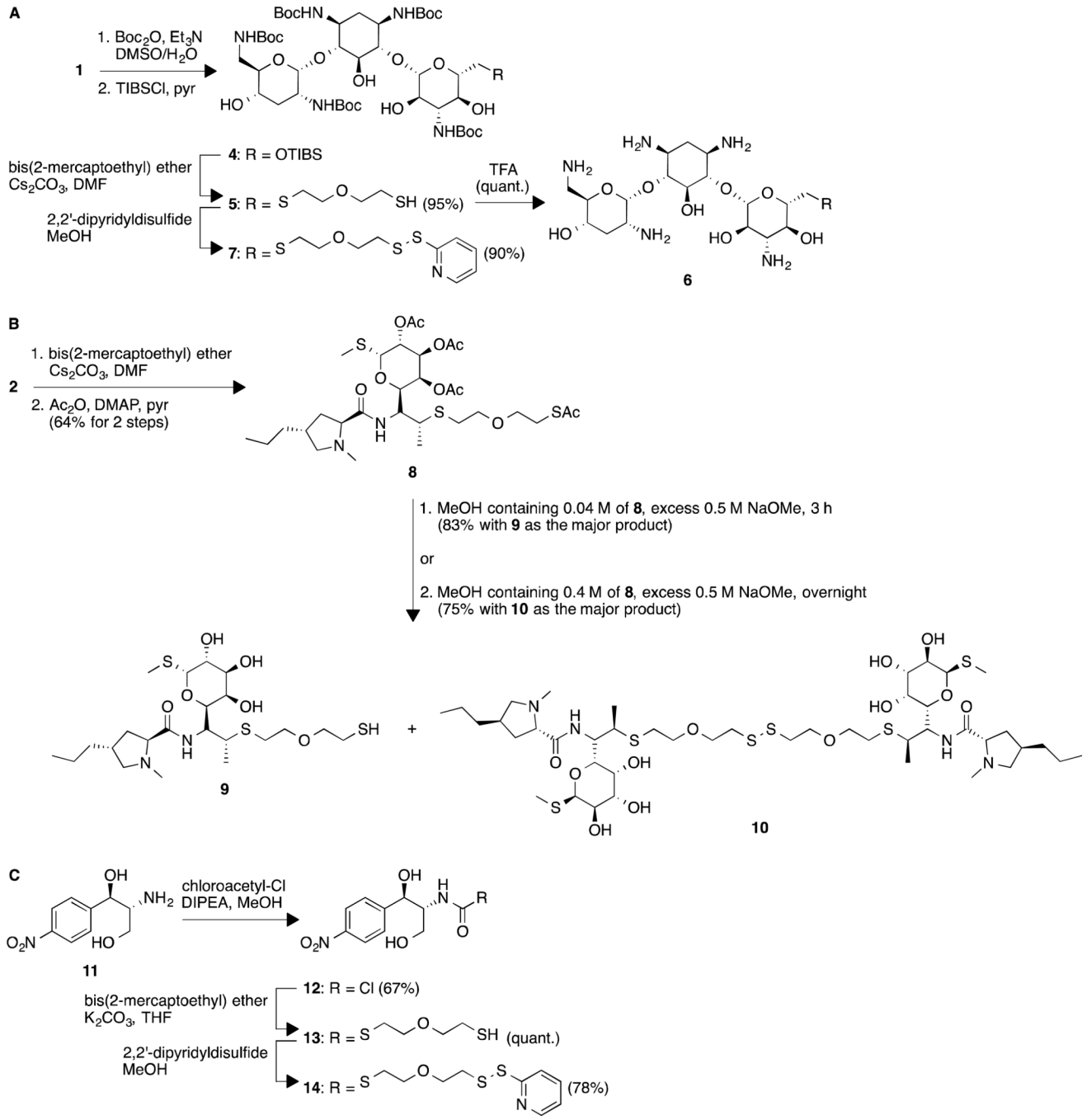

Scheme 1.

Synthetic schemes for the preparation of **A**. Tobramycin monomer building blocks, **B**. Clindamycin monomer building block and of clindamycin-clindamycin dimer **10**, and **C**. chloramphenicol monomer building blocks.

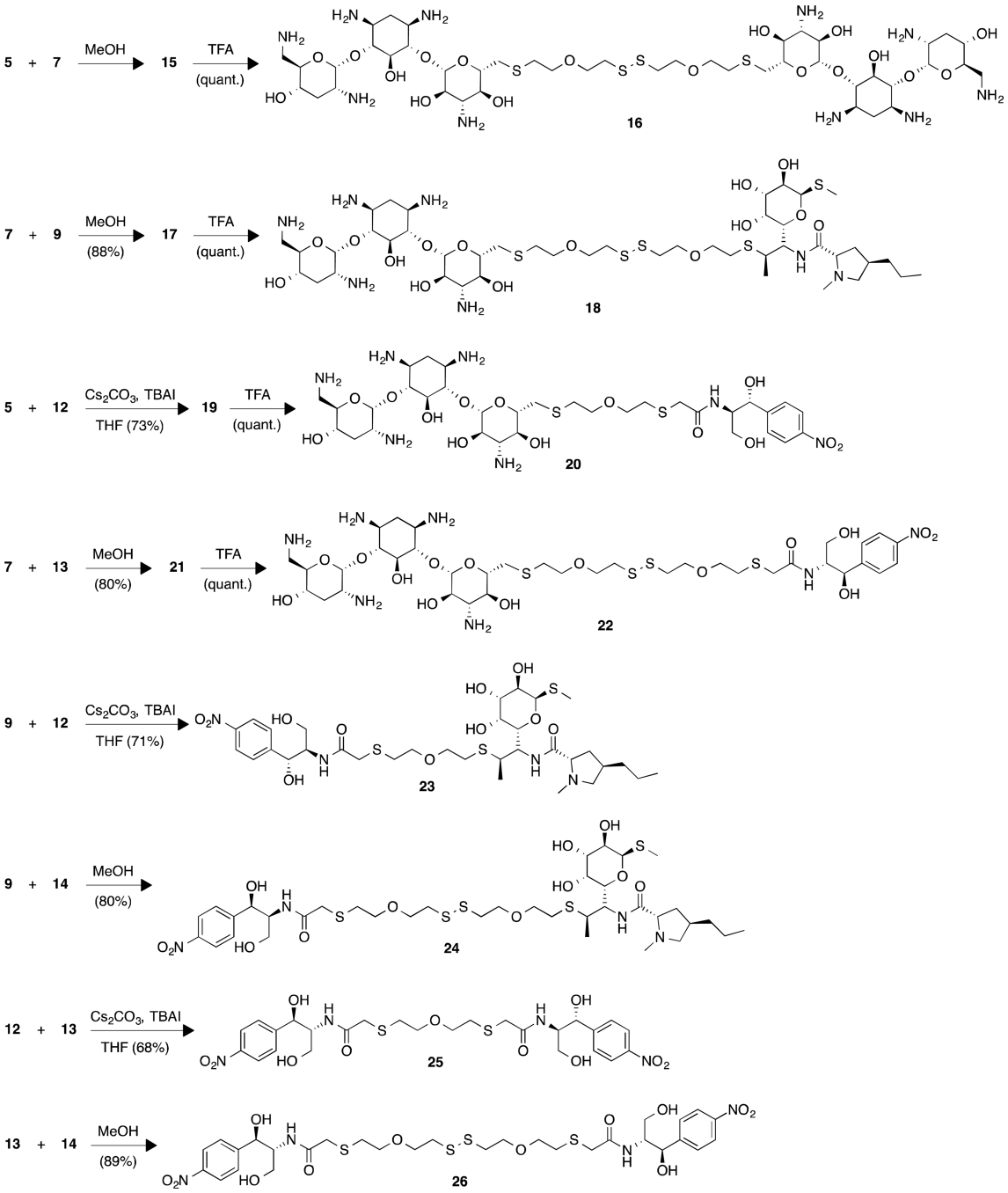

Scheme 2.
Synthetic scheme for the preparation of homo- and hetero-dimers derived of **1, 2**, and **3**.

J Med Chem. Author manuscript; available in PMC 2014 July 11.

Table 1

Antibacterial activity of homo- and hetero-dimers and parent AGs against Gram-positive (+) and Gram-negative (−) bacterial strains[a]: MIC values (μg/mL).

Cpd #	A (+)	B (+)	C (+)	D (+)	E (+)	F (+)	G (+)	H (−)	I (+)	J (−)	K (+)	L (+)
Parent drugs												
1	2.3	9.4	0.6	75	18.8	37.5	9.4	9.4	9.4	18.8	0.3	64
2	0.6	>150	9.4	1.2	4.7	0.6	<0.3	2.3	<0.3	4.7	1	1
3	2.3	1.2	18.8	4.7	9.4	9.4	4.7	<0.3	4.7	0.6	8	4
Parent compounds with linker												
6	2.3	75	2.3	150	18.8	75	18.8	18.8	37.5	37.5	16	128
9	9.4	>150	75	9.4	37.5	4.7	1.2	37.5	2.3	75	4	2
13	>150	>150	>150	150	>150	>150	>150	37.5	150	>150	>128	128
Homo-dimers												
10	2.3	>150	18.8	2.3	4.7	0.6	0.6	9.4	2.3	37.5	1	>128
16	0.6	37.5	2.3	75	37.5	37.5	9.4	18.8	37.5	9.4	16	64
25	>150	>150	>150	>150	>150	>150	>150	>150	>150	>150	>64	>128
26	150	>150	>150	75	9.4	0.6	>150	18.8	75	150	>64	>128
Hetero-dimers												
18	1.2	150	4.7	9.4	18.8	2.3	4.7	4.7	2.3	75	2	64
20	150	>150	18.8	>150	>150	>150	>150	>150	>150	150	8	8
22	4.7	150	4.7	150	18.8	150	9.4	4.7	75	37.5	16	16
23	18.8	>150	>150	18.8	75	18.8	18.8	9.4	2.3	75	4	>128
24	2.3	>150	18.8	2.3	4.7	0.6	<0.3	4.7	<0.3	150	2	>128

[a] *B. subtilis* 168 (A), *B. subtilis* 168 with AAC(6')/APH(2")-pRB374 (B), *M. smegmatis* str. MC2 155 (C), *B. cereus* ATCC 11778 (D), *L. monocytogenes* ATCC 19115 (E), *S. aureus* ATCC 29213 (F), *S. aureus* NorA (G) *E. coli* MC1061 (H), *B. anthracis* 34F2 Sterne strain (I), *H. influenzae* ATCC 51907 (J), *S. epidermidis* ATCC 12228 (biofilm negative) (K), and *S. pyogenes* serotype M12 *str*. MGAS9429 (L).

Table 2

Activities of homo- and hetero-dimers and parent AGs in an *in vitro* prokaryotic translation assay.

Compound #	IC_{50} (μM)
Parent drugs	
1	0.015 ± 0.001
2	18.1 ± 0.8
3	6.4 ± 0.4
Parent compounds with linker	
6	0.43 ± 0.01
9	>100
13	48.7 ± 1.8
Homo-dimers	
10	6.1 ± 1.1
16	0.27 ± 0.01
25	32.9 ± 2.6
26	25.6 ± 2.1
Hetero-dimers	
18	0.98 ± 0.05
20	1.49 ± 0.05
22	1.00 ± 0.16
23	14.7 ± 1.2
24	18.3 ± 0.3